Quantifying Hydrological Connectivity in the Trinity River Delta

Texas Water Development Board Contract #2000012435

Nelson Tull

Paola Passalacqua, PhD

Ben Hodges, PhD

The University of Texas at Austin

May 2023

Pursuant to Senate Bill 1 as approved by the 86th Texas Legislature, this study report was funded for the purpose of studying environmental flow needs for Texas rivers and estuaries as part of the adaptive management phase of the Senate Bill 3 process for environmental flows established by the 80th Texas Legislature. The views and conclusions expressed herein are those of the author(s) and do not necessarily reflect the views of the Texas Water Development Board.

Contents

List of Figures

List of Tables

Executive Summary

This study combines field data collection and numerical modeling for the purpose of understanding the mechanisms of flow exchange between the lower Trinity River and its floodplain, particularly as it approaches the coast. We performed three field campaigns, in May 2022, October 2022, and April 2023 during medium, low, and high flow conditions, respectively. For each campaign, we took discharge measurements using an Acoustic Doppler Current Profiler (ADCP) at different locations along the river to see where flow was moving between the river and floodplain. During May 2022, we also placed six pairs of sensors in the floodplain to measure water levels and flow velocities in the smaller floodplain channels that were dry during the first two field campaigns but can become inundated during higher flow events. From the ADCP data we were able to quantify the flow rates moving through several of the larger floodplain channels, and show that these channels are important conduits for river-floodplain exchange and delta flow circulation at all discharges. The ADCP data also showed the ways in which the gate and dam in Wallisville, TX, operated by the U.S. Army Corps of Engineers (USACE), controls the hydraulics of the Trinity River. We calibrated a numerical model using the ADCP data and U.S. Geological Survey (USGS) gaging stations in the area, and used it to quantify how surface-water connectivity between the river and floodplain changes as the river approaches the coast and as discharge increases from sub-bankfull to bankfull. We then coupled a passive tracer model to our hydrodynamic model to discover which river bends and floodplain channels convey the largest fluxes between the river and floodplain. Through this analysis we emphasize the complex ways in which river water can move to and from the floodplain, both through individual floodplain channels and also across local river banks that are unbounded by natural levees. Model results and the ADCP data both illustrate the importance of the topographic bluffs that constrict the floodplain at three locations within the study area. Floodplain flow volumes and fluxes alternate in magnitude based on proximity to the bluffs, as flow is forced to re-enter the river upstream of each bluff. We anticipate that the data and results from this study will provide insight into the important natural and human-made features of the lower Trinity River system that influence flow hydraulics near the Trinity Bay.

Plain Language Summary

This study presents an analysis of river and floodplain flows along the Trinity River between Liberty, TX and Trinity Bay. We collected measurements of river flow rate in May 2022, October 2022, and April 2023. River flows varied considerably among these three measurement campaigns. We measured flow rates at many locations to observe how the river flow was changing along the length of the river. In general, when river flow was high (April 2023), there were many locations along the river where flow was moving from the river into the floodplain, and vice-versa. Very little flow moves between the river and floodplain when river flow is low (e.g., in October 2022), with the exception of the Trinity Bay region, where the tides interact with the river flow to move water through the network of delta channels there. In most cases, locations of flow "loss" or "gain" were occurring through floodplain channels, or other gaps in the river bank, that are low enough in elevation to convey water between the river and floodplain even when the river water level is below the elevation of the river bank. In addition to river flow measurements, we also placed water level and velocity sensors in several of these floodplain channels to get a sense of how much water moves between the river and floodplain at various river stages. The river flow measurements show how the gate and dam at Wallisville, TX, operated by the U.S. Army Corps of Engineers (USACE), influence flow patterns in the study area. We also developed a computer model of the study area, inspired by the collected data, to further understand the flow patterns occurring in the system. Our model results describe the complexity of flow directions and flooding patterns in the Trinity River floodplain. A key finding from the field data and model is on the importance of topographic bluffs, or locations of high elevation immediately adjacent to the river. These bluffs effectively disconnect the floodplain upstream of the bluff from the floodplain downstream. This disconnection forces water in the floodplain to return back to the river through one or more floodplain channels, located just upstream of the bluff. Understanding how water flows in and out of the river under different flow conditions is important for water resource managers, floodplain managers, ecologists, and river engineers.

Acknowledgements

This work was supported by the Texas Water Development Board (TWDB) under contract 2000012435 to the University of Texas at Austin. This study was conducted by Nelson Tull as part of his ongoing PhD work, supervised by Dr. Paola Passalacqua and with guidance of dissertation committee member Dr. Ben Hodges. The authors thank Dan Duncan and Marcy Davis from the University of Texas Institute of Geophysics (UTIG) for their help in collecting river discharge data. The authors also thank Dr. David Mohrig, Dr. Andrew Moodie, and PhD student Mariel Nelson for their help with field work and development of the modeling approach.

1 Introduction

The main channel and floodplain of the lower Trinity River (Texas, USA) undergoes significant topographic and hydraulic change between the towns of Romayor and Wallisville (Figure 1). For the most part, the floodplain over this distance of about 78 river miles (125 km) is still in its natural state, with the exception of a few dirt access paths, abandoned oil fields, and a few sparse dwellings. The river is free to migrate and develop levees, which has resulted in the development of a variety of pathways, or floodplain channels, that connect the river and floodplain and bring water, sediment, and nutrients to the floodplain. These geomorphic processes and characteristics change, however, as the river approaches the coast, largely due to the river's transition from uniform to backwater-dominated flow (Smith et al., 2020). Channel migration rates are significantly lower in the backwater reach, and the natural river levees are much more pronounced (Hassenruck-Gudipati et al., 2022). Therefore, the number, size, and orientation of the floodplain channels connecting the Trinity River and its floodplain change with distance downstream.

It is likely due to these topographic and hydraulic changes along the river that there is an obvious signature of flow loss from the main river between the U.S. Geological Survey (USGS) gaging stations at Romayor (USGS 08066500) and Wallisville (USGS 08067252), particularly during high flow events (Figure 2). Over the five-year period shown in Figure 2, the USGS record indicates only half the volume of water that passed by Romayor also passed through the river at Wallisville. Even under lower flow conditions, aerial imagery provides evidence of numerous locations of surface-water connectivity between the river and floodplain, and that the number and size of inundated channels increases toward the coast (see Figures A.1-A.4 for examples of surface-water connectivity from upstream to downstream). Understanding the volumes of water that flow through the river and floodplain under low flow conditions is important for the management of water resources and ecosystems along the river. Under high flow conditions, understanding the mechanisms behind the increased flow to the floodplain is essential for flood management, and also ecosystem services and sediment transport in the system.

The goal of this study was to determine the locations and mechanisms of flow loss from the Trinity River main channel upstream of the U.S. Army Corps of Engineers (USACE) control structure at Wallisville, as well as flow partitioning in the delta downstream of Wallisville. This work is inspired in part by previous work performed on the Wax Lake Delta in Louisiana (Hiatt and Passalacqua, 2015). We combined field measurements taken during three field campaigns with a hydrodynamic model to analyze the distribution of flows moving through the Trinity River and floodplain, and how that distribution changes at low, medium, and high river discharges. In Section 2, we introduce the numerical model used in this study. In Section 3, we describe the scope of our three field campaigns in May and October of 2022 and April of 2023, and the data collected during those campaigns. In Section 4, we describe a modeling approach informed by the field measurements, and a few ways that the model was used to gain insight into river-floodplain flow dynamics. Lastly, in Section 5 we discuss our most important findings and their implications.

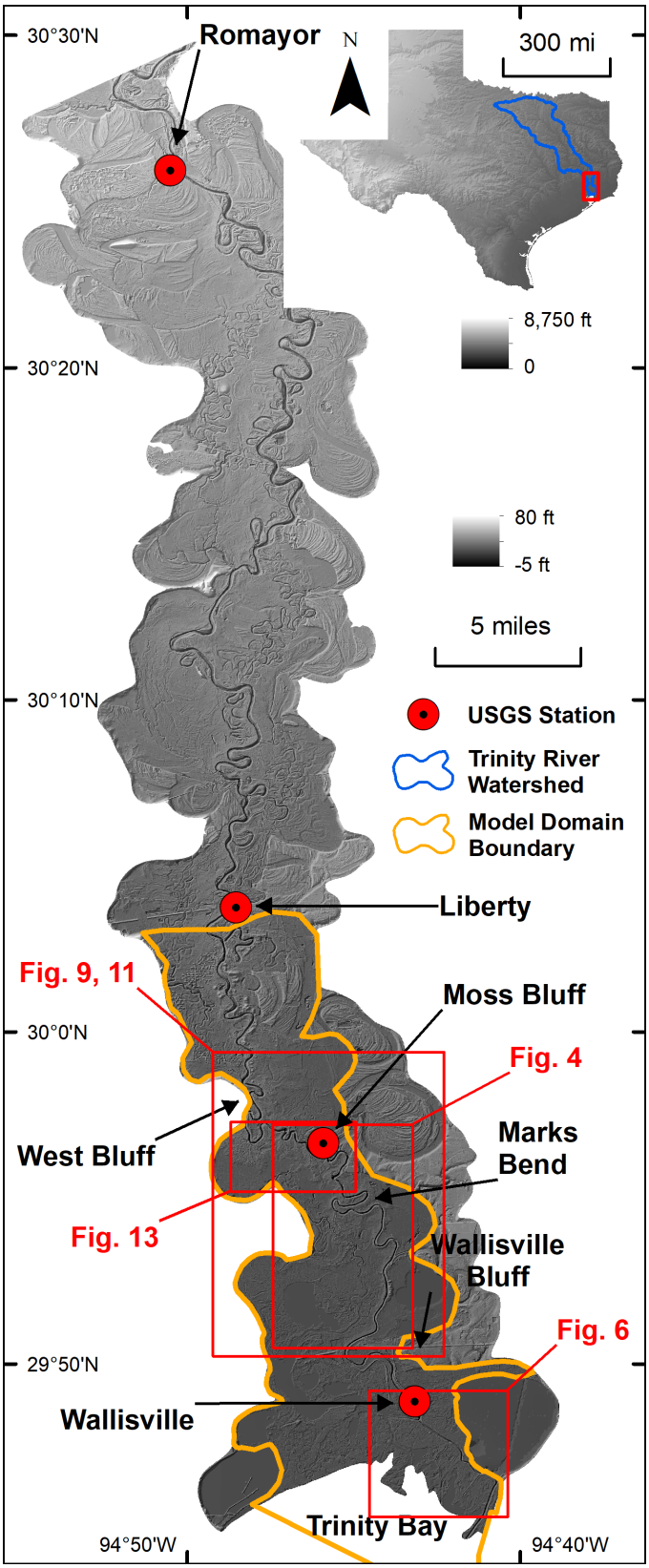

Figure 1: Elevation map of the lower Trinity River, including domain boundary used for numerical model. Red boxes indicate spatial extents for several subsequent figures in this report.

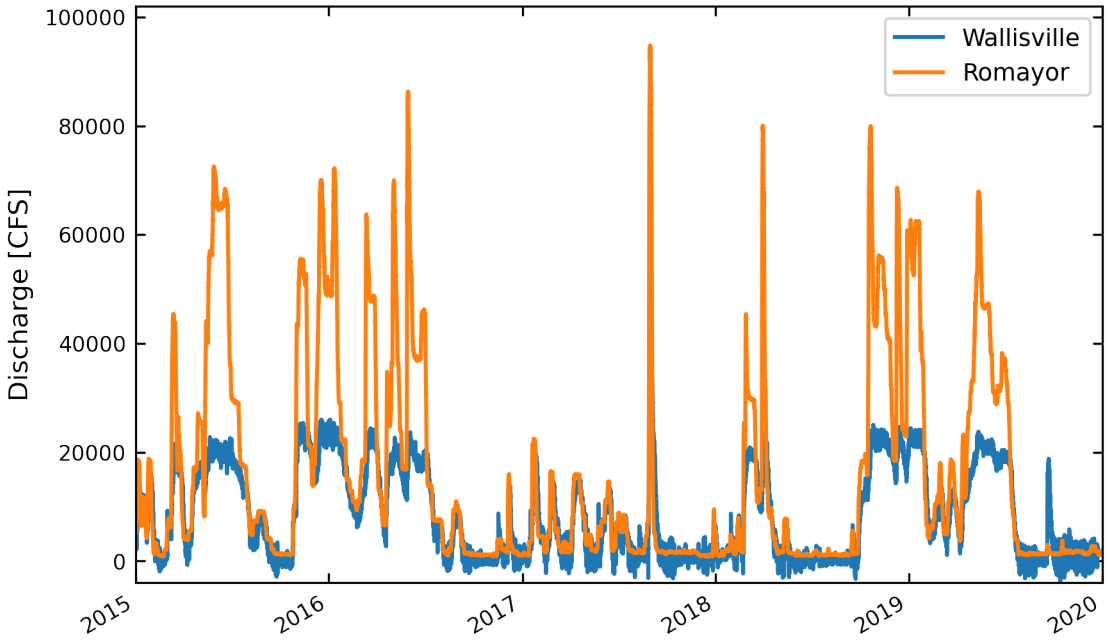

Figure 2: Time series of water discharge at two USGS gaging stations on the Trinity River: Wallisville (USGS 08067252) near the Trinity River delta and Romayor (USGS 08066500), far upstream.

2 Using a Numerical Model to Inform Field Investigations

2.1 Elevation Data

All elevation data and references to elevation in this report are relative to the NAVD88 datum. The elevation data shown in Figure 1 and others were derived from lidar measurements collected in February and March of 2017 as part of the Texas Strategic Mapping Program (https://tnris.org/stratmap/). Data were acquired and processed by the Sanborn Map Company through funding from the Texas Water Development Board, with third-party quality assurance and control provided by AECOM. Collection took place during the leaf-off season in Texas. The reported horizontal and vertical accuracy of the lidar are 0.25 m (0.82 ft) and 0.29 m (0.95 ft), respectively.

The lidar data were interpolated to a bare-earth digital elevation model (DEM) at 1-m (3.28 ft) resolution. Small voids in the floodplain lidar were interpolated using a second-degree polygon plane fit through the existing data. River bathymetry measurements were taken by the Trinity River Authority in 2017, along four longitudinal profiles at transects spaced every 1,300 ft (400 m) on average (the river width varies between 260 and 330 ft). The bathymetry was interpolated to a 10-m (32.8 ft) grid, and patched together with the lidar DEM using the Raster to Mosaic tool in ArcGIS. Finally, linear interpolation was performed across the small gaps between the lidar DEM and bathymetry raster.

2.2 Preliminary Modeling with ANUGA

We used the Australian National University and Geosciences Australia (ANUGA) hydrodynamic model for numerical modeling in this study. ANUGA is an open-source model developed by researchers at the aforementioned institutions (Roberts et al., 2015). It solves the shallow-water equations using unstructured meshes and a finite-volume numerical scheme (Mungkasi and Roberts, 2011). ANUGA is the model of choice for several reasons, including: (*i*) it is open-source and therefore easy to control and customize; (*ii*) the finite-volume method conserves mass and momentum along the wetting-drying front; (*iii*) it uses unstructured meshes; (*iv*) it scales efficiently in high performance computing environments; and (*v*) it employs a variable time step. The flexibility of the unstructured mesh allows for higher mesh resolution in priority areas, while offering reduced resolution in areas of less concern. The unstructured mesh, along with the parallel capabilities and variable time step, reduces the computational resources needed for model simulations, which is important for large-domain applications where high mesh resolution is employed in some areas. ANUGA was originally developed for coastal applications such as tsunami modeling and has been validated for such applications (Mungkasi and Roberts, 2013; Nielsen et al., 2005). In recent years, ANUGA has been used for delta and coastal river systems along the U.S. Gulf Coast and other similar applications (Hariharan et al., 2023; Tull et al., 2022; Wright et al., 2022a,b).

We ran a handful of preliminary model simulations that focused on understanding discharge in the main channel in the region between Moss Bluff and Wallisville (see Figure 1 for locations). Model output showed that, for discharges over about 10,000 CFS (300 m^3/s), there could be significant flow loss from the main channel upstream of Wallisville and the delta region. At medium discharges (between about $10,000 - 18,000$ CFS, or $300 - 500$ m^3/s) the model showed that the majority of flow loss actually occurs at a sinuous set of river bends in the backwater reach, known as "Marks Bend" (Figure 1). Marks Bend is a unique feature of the river and is notable for several reasons, in addition to its high sinuosity (which is unmatched elsewhere along the river). First, there is a large distributary channel known as "the Cutoff" connected to it, which is deep enough to be connected hydraulically to the river even at low flows. Second, the northern banks of the channel at Marks Bend are unbounded by levees, while the southern banks have well-developed levees similar to most other channel banks in the backwater reach. The likely reason for this structure is the general north-south direction of river flow, where the north-south flow momentum at high river discharge would be more likely to advect sediment over the southern banks than the northern banks. The implication is that the lack of prominent levees on the northern banks may allow for river water to pass into the floodplain at lower discharges compared to other locations in the backwater reach.

Our preliminary modeling helped to inform our understanding of Marks Bend as a location of potential flow loss from the Trinity River under medium discharges. We developed a more robust numerical model following our collection of discharge data during our field campaigns, which was partly inspired by the data we collected. Details on model development and inputs are provided in Section 4.

3 Overview of Field Campaigns

3.1 ADCP Measurements

In May and October of 2022 and April of 2023, we performed field campaigns on the Trinity River that involved taking river discharge measurements with an Acoustic Doppler Current Profiler (ADCP). Discharge measurements were performed using the RiverRay ADCP from Teledyne Marine. The ADCP was mounted on the bow of the R/V Scott Petty, a research vessel operated by the University of Texas Institute for Geosciences (https://ig.utexas.edu/facilities/rv-scott-petty/). Data were collected and stored using the WinRiver II software. At each transect, we began on one side of the river and moved across the river as close to perpendicular to the flow direction as possible. The start and end position of each transect were located on average about 30 feet from the adjacent river bank, to avoid getting stuck in vegetation and shallow waters. We used a Laser Rangefinder to estimate the horizontal distance from the end of the transect to the river bank. WinRiver uses standard methods for extrapolating the velocity measurements to account for each missing edge of the cross section, in addition to estimating the discharge in the top and bottom layers of the cross section where the ADCP is not able to accurately measure velocity.

Flows in the Trinity River were low for the majority of 2022 (Figure 3A), compared to previous years. Fortunately, during our planned field dates of $11-12$ May 2022, the river discharge of about 13,000 CFS (370 m^3/s) was higher than it had been for the majority of the previous winter and spring (Figure 3B). During the dry seasons of summer and fall, flows were low and generally between 1,000 and 1,800 CFS (30 and 50 m^3/s), with the exception of a brief pulse of water that resulted from the heavy rains experienced in the Dallas-Fort Worth area in late August 2022. The river discharge during our second field campaign ($19-20$ October 2022) was low and nearly constant at about 1,400 CFS (40 m^3/s, Figure 3C). The higher discharge during the first field campaign provided an opportunity for surveying the river upstream of Wallisville, while the lower discharge in October provided conditions for surveying the delta, where tides would be more influential and water flow through the many distributaries is in general less dependent on river discharge. Spring 2023 brought greater flows to the river, particularly during the months of April and May. During our third and final campaign (13 April 2023), river discharge peaked at 28,800 CFS (820 m^3/s, Figure 3D), allowing for an environment where flows were being exchanged between the river and floodplain at many locations.

The following sections present the ADCP data collected during each of the three field campaigns. Throughout the presentation of these data, we describe changes in river discharge at various locations along the length of the river. Each of the described changes in river discharge is accompanied by a percent value; this value is the flow exchange between the river and floodplain as a percentage of the known discharge at the Liberty USGS gage (USGS 08067000) upstream at that point in time. Also note that values of discharge are rounded for simplicity and to reflect uncertainties in the measurements. Some values discussed in the following sections may not match exactly the values shown in tables, particularly following instances where multiple values are added together.

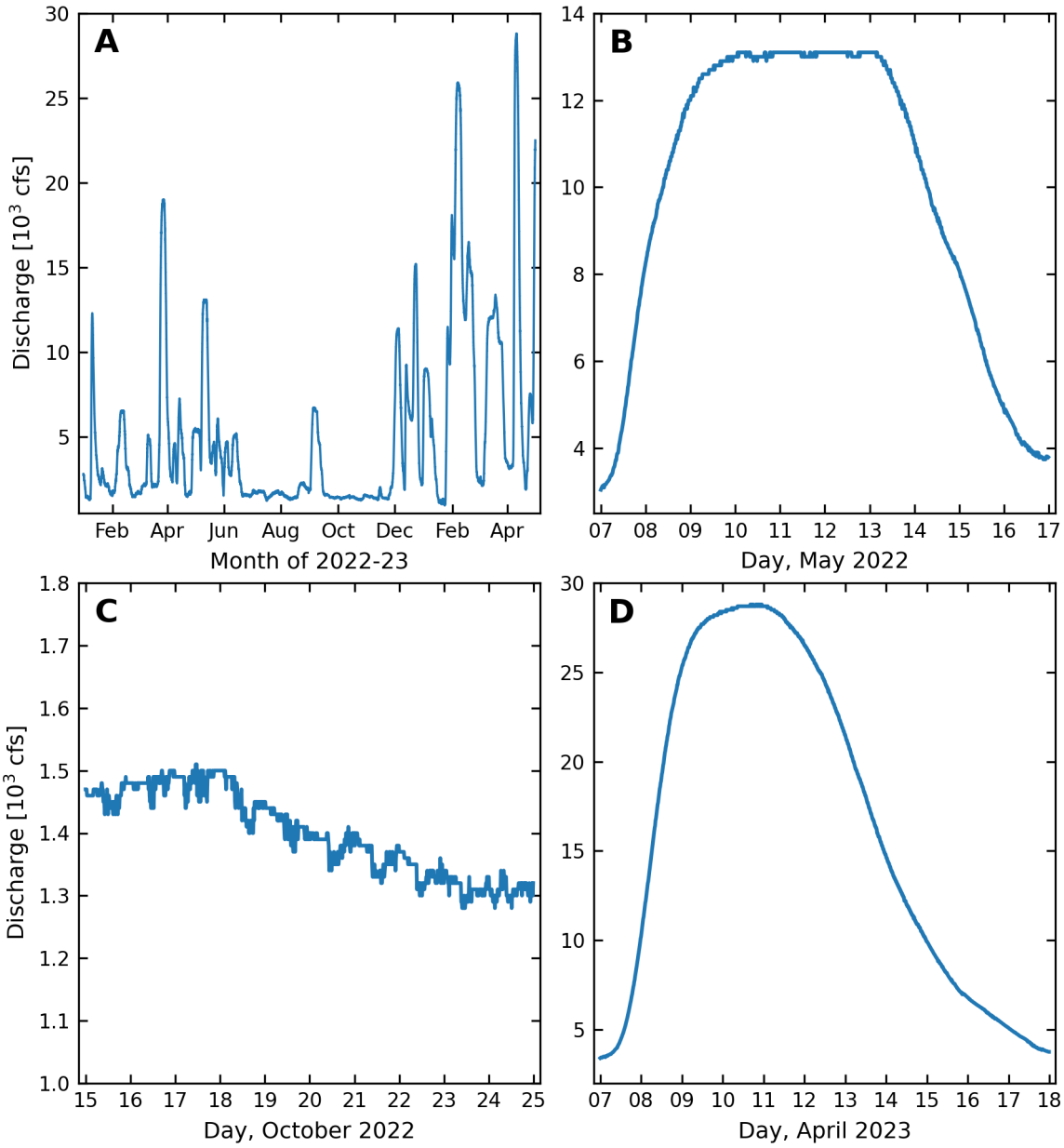

Figure 3: (A) Hydrograph of the Trinity River at USGS 08067000 in Liberty, TX for the year 2022 and first four months of 2023. (B) Hydrograph during the May 2022 campaign. (C) Hydrograph during the October 2022 campaign. (D) Hydrograph during the April 2023 campaign.

3.1.1 May 2022 Campaign

ADCP measurements during the first field campaign were taken at many locations along the river upstream of Wallisville during 11−12 May 2022 (Figure 4), with a focus on Marks Bend. The transects shown in Figure 4 are numbered in increasing order from upstream to downstream, where transects $1-14$ were planned and the other transect measurements were taken due to extra time available. At each of these transects, we took at least three discharge measurements, and in most locations we took four. USGS standards recommend an even number of two or more measurements at each transect for sufficient averaging. At transects where we took only three measurements, we averaged together the

two measurements of the same direction prior to averaging with the third measurement, to account for any directional bias. The exception is transect "B", which has only one associated measurement. Measurements at transects A – F were taken because they are adjacent to the sites in the floodplain where we performed additional field work (see Section 3.2), and because they would provide insight into the river discharge upstream in the vicinity of a few larger floodplain channels. Transects 15 – 18 were included to measure the net flow into the river through the two major floodplain channels at those locations, where we did not have prior knowledge of flow directions (into or out of the river).

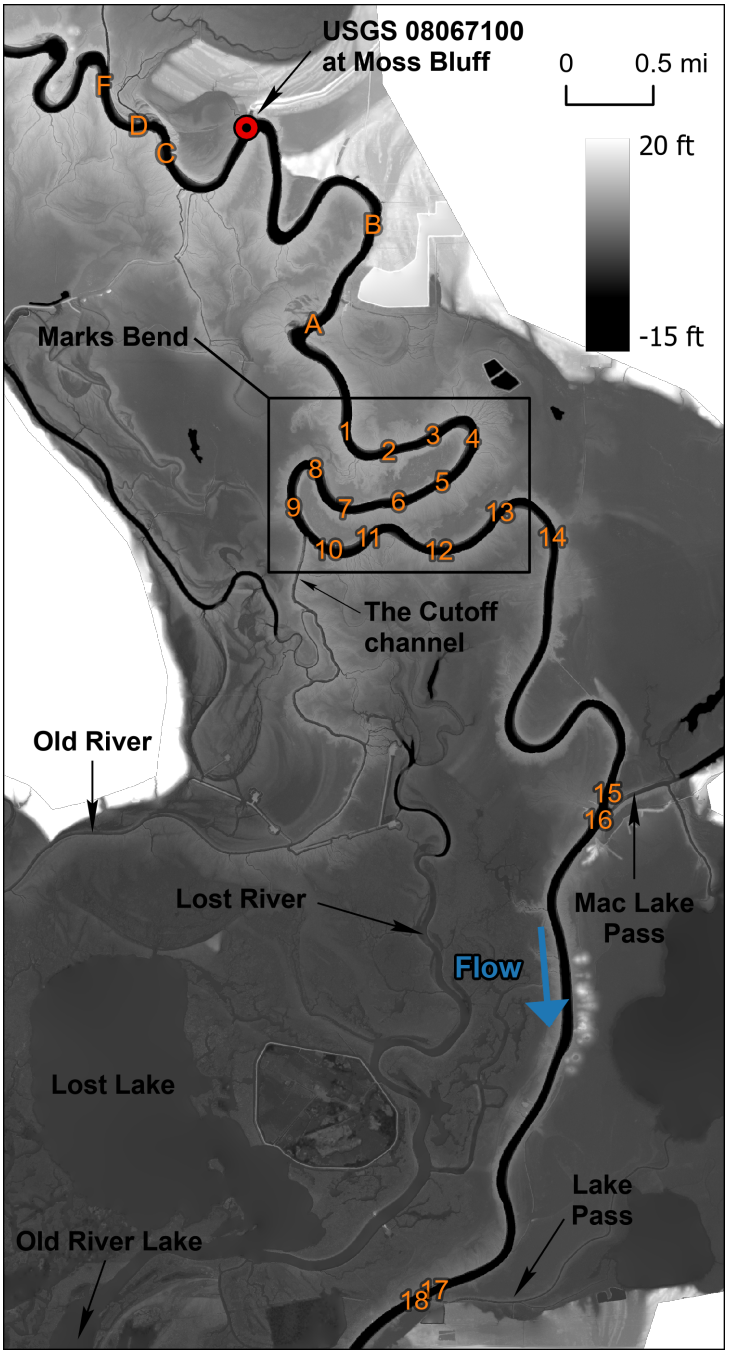

Figure 4: Location of ADCP transects taken during the field campaign in May 2022.

Discharge data collected during this campaign are shown in Figure 5. During both days

of collection, the discharge at the Liberty gage upstream was about 13,000 CFS (370 m^3/s). The data collected between transects F and 9 show that the discharge in the river is generally between $10,900 - 11,300$ CFS ($310 - 320$ m^3/s), which is significantly lower than the discharge at the Liberty gage. There are a few locations upstream of this study site where there was likely to be flow moving from the river to the floodplain at these discharges, and because the higher discharge period had only began $2 - 3$ days prior (Figure 3B), it is possible that water was still actively flowing out of the river at those locations. However, much of the discharge gap between the Liberty gage and our study area could be due to pumping by the Coastal Water Authority (CWA) at the bluff just upstream of a dirt access path known as "Camp Road" (Figure 4). The CWA pumps continuously at an average rate of 920 CFS (26 m^3/s) from this location, and is an important source of flow loss in this part of the Trinity River system (see USGS 08067070 for daily pumping rates).

Between transects 9 and 10, there is an obvious drop in discharge of 1,160 CFS (33 m^3/s, 9%) measured in the river. This flow reduction coincides with the Cutoff channel (Figure 4, Figure B.1). The Cutoff is one of the starting points of the Lost River and Old River, both of which combine to form two major lakes in the floodplain and delta: the Lost Lake and Old River Lake (Figure 4). Thus, it is not surprising that there was a substantial reduction in flow beyond this distributary. There are two other large floodplain channels of similar size that connect to the river downstream of Marks Bend, one at transects $15 - 16$ and the other at transects $17 - 18$, the latter of which is located just upstream of Interstate-10 and the USACE control structure. At the first channel (unnamed, so we refer to it as "Mac Lake Pass"), we found that flow was moving out of the river at a rate of about 413 CFS (12 m^3/s, 3%). We were surprised by this flow direction because the confluence angle of the floodplain channel is more indicative of a tributary, but it was confirmed by ADCP velocity vector readings within the channel itself. This channel flows between the river and system of several floodplain lakes, and likely conveys water to those lakes from the river during periods of higher discharge. The floodplain channel at transects $17 - 18$ ("Lake Pass") also connects to a system of floodplain lakes, but in this case the ADCP indicated water flowing into the river. However, flow velocities in Lake Pass were much smaller than in Mac Lake Pass, and the ADCP transect measurements show a negligible increase in river flow at this location (Figure 5). Instead, the measurements show a greater discharge increase of 310 CFS (9 m^3/s, 2%) over the distance between Mac Lake Pass and Lake Pass, which could be a result of flow moving overbank at certain locations along this reach where the bank line is low in elevation. However, we did not observe any such flow locations as we traversed between transects 16 and 17.

3.1.2 October 2022 Campaign

We performed another set of ADCP measurements on 20 October 2022, this time in the Trinity River delta region farther downstream (Figure 6). Because of the low river discharge during this time (1,400 CFS, 40 m^3/s, Figure 3C), it was unlikely that any of the floodplain channels in the previously measured reach would be as active, and thus it was more likely for discharge to remain mostly constant along the river. The delta region downstream of Wallisville consists of many distributaries with flow magnitudes and directions that are likely influenced by both river discharge and tides. We took discharge measurements from Wallisville to Anahuac, beyond which there are no more

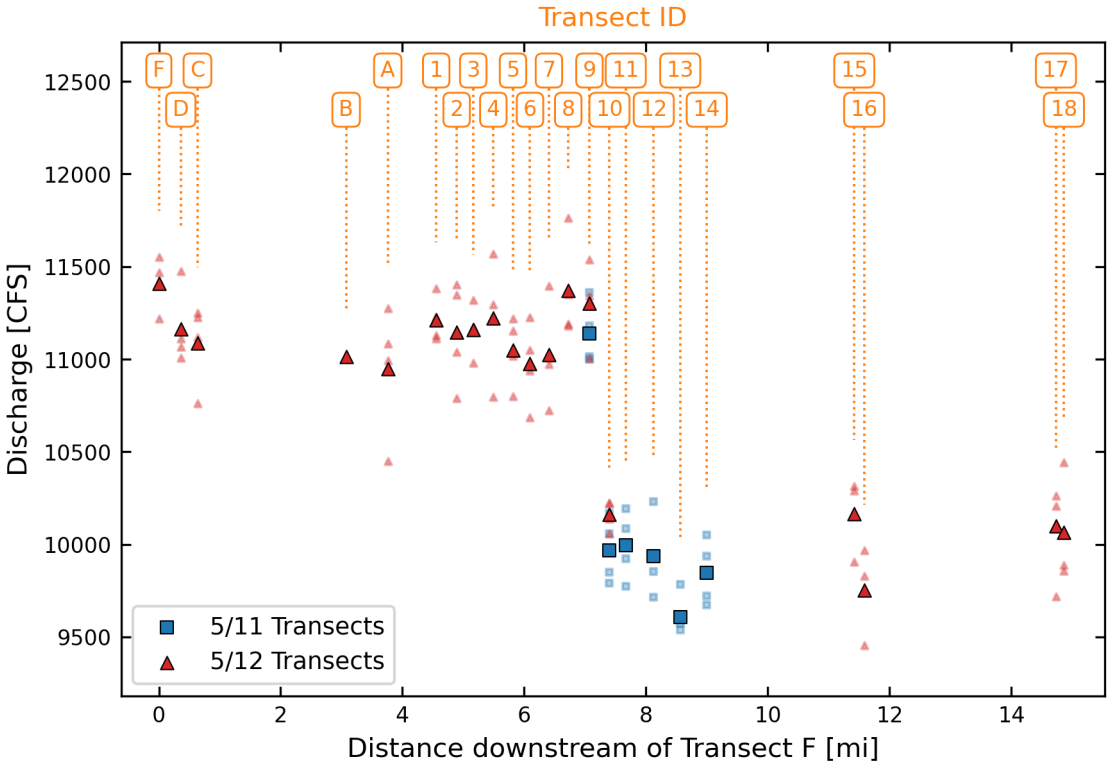

Figure 5: River discharges measured at each transect visited on 11 – 12 May 2022, with transect labels shown at the top corresponding to those in Figure 4. The lightly colored markers indicate individual measurements, while the solid, larger markers indicate the mean value. The reference discharge at the Liberty gage during the two days of measurements was 13,000 CFS (370 m^3/s).

major distributary channels connecting the Trinity River to the bay. Our goal was to understand how the flows downstream of Wallisville are distributed through the many connected delta channels, or "passes", as well as the influence of tides through the delta.

The USACE gate at Wallisville (channel "D1" in Figure 6) is kept closed during periods of low river discharge to prevent excessive saltwater intrusion into the river and floodplain upstream. The river splits in two at this location, and on the opposite branch there is a "run-of-river" dam (channel "D2" in Figure 6). Upstream of this set of structures, the river and floodplain are separated by engineered embankments that extend up to Interstate-10. Although the gate was closed during our field campaign, it is allowed to open once every hour for boat traffic that requests it. When we passed upstream of the gate at 1200 CDT on 19 October, we estimate that there was a head difference of $2 - 3$ feet. The operation of this structure is certainly an important aspect of the hydraulics of the Trinity River.

The transects shown in Figure 6 are generally located in such a way that they represent conditions in the river before and after a change in flow is expected due to the presence of a distributary channel. Transects D1 and D2 represent the fraction of flow in each branch of the channel at the USACE split, while transects D3 and L1 represent the fraction of flow continuing down the main channel versus flowing into the Old River to the west. Transect L2 is in the same channel as L1 but was measured at a later time, and transect

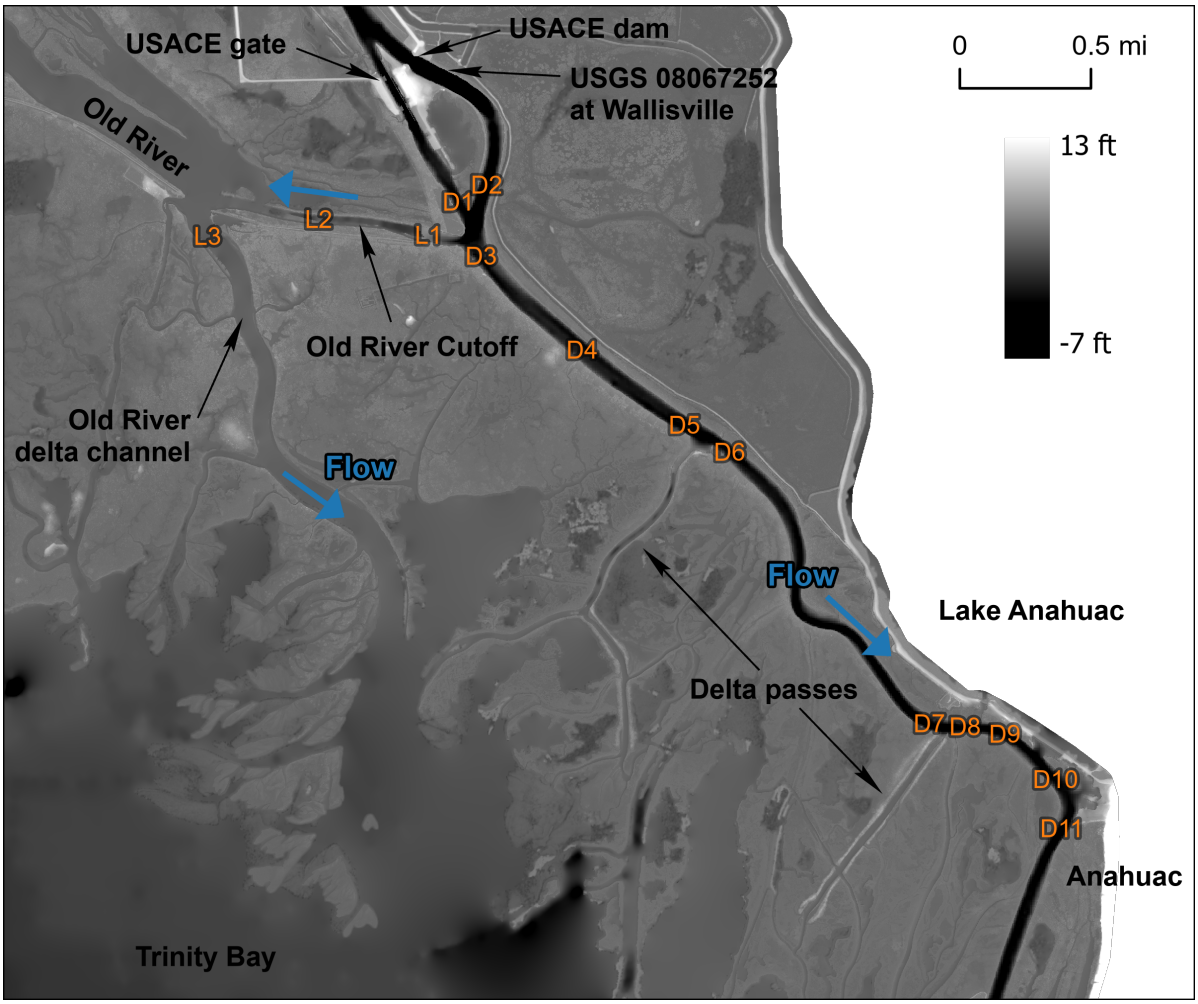

Figure 6: Location of ADCP transects taken during the field campaign in October 2022. Transects D1, D2, D3, L1, and L3 were repeated during the April 2023 campaign.

L3 is located in a large channel that has its own delta building out into the bay, which indicates this channel conveys a significant amount of fluvial water and sediment.

Discharge measurements in the delta are shown in Table 1. Measurements began at transect D1 at 1020 CDT, approximately 2.5 hours after high tide. The final measurement was taken at the same transect at 1515 CDT, approximately halfway between high tide and the lowest tide (see Figure 7 for orientation on tidal period). Southwesterly winds from the bay increased the difficulty of many of the measurements, particularly those farther downstream closer to the bay. Furthermore, one of the two engines on the boat was incapacitated during this field campaign, which made navigation along the transects difficult and travel time between transects much longer than usual. Discharge measurements shown in Table 1 should be interpreted with these factors in mind.

Although flows did not change much over the length of the main channel (transects D3 – D11), the data in Table 1 still provide several insights. First, flow through the west channel downstream of the USACE gate (transect D1) was much less than the flow through the east channel downstream of the dam, because the gate was closed and therefore most flow was passing through the dam. However, it is worth noting that there is still a minimum flow rate through the gate even when it is closed. Second, the flow

Table 1: Discharges measured at each transect visited on 20 October 2022, with transect labels corresponding to those in Figure 6 (all discharges in units of CFS). The reference discharge at the Liberty gage when these measurements were taken was 1,400 CFS (40 m^3/s).

Transect	Time (CDT)	No. Measurements	Mean	Min	Max
D1-A	1020	3	179	173	191
D1-B	1515	2	94	60	173
D2	1503	3	769	717	805
D3	1343	2	1040	964	1070
D4	1323	3	1060	999	1110
D5	1306	3	1200	1170	1230
D6	1253	3	1280	1240	1330
D7	1226	3	1250	1190	1310
D8	1212	3	1160	1070	1200
D9	1159	3	1110	1050	1220
D10	1145	3	1060	999	1090
D11	1134	3	1150	1030	1240
L1	1359	2	385	378	392
L2	1443	3	574	512	650
L3	1423	4	2530	2510	2590

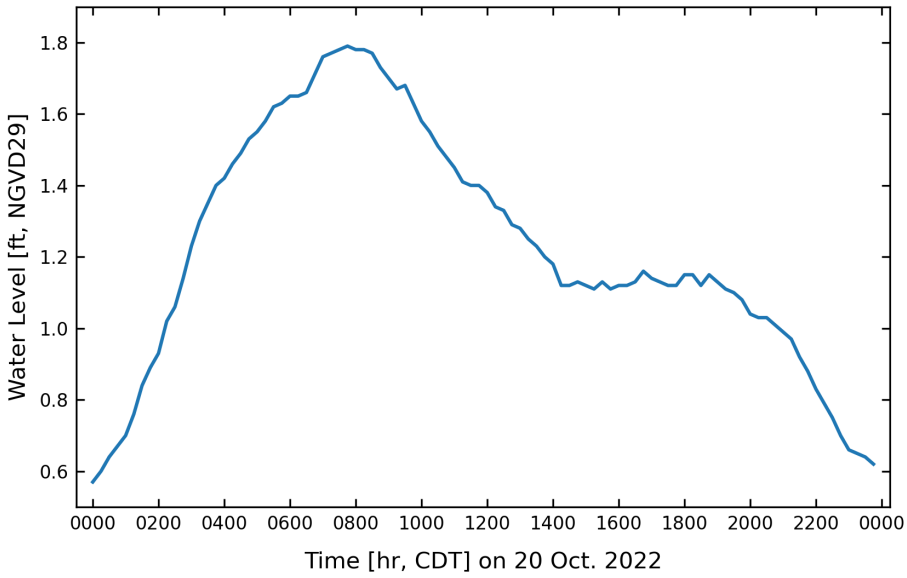

Figure 7: Water level recorded at Wallisville (USGS 08067252) on 20 October 2022. Note that the datum of the Wallisville gage is NGVD29, but in this location NGVD29 and NAVD88 datums are nearly equivalent.

increased by about 241 CFS (7 m^3/s, 17%) from transects D3 – D6 and then decreased again from transects D6–D8 by about 116 CFS (3 m^3/s, 8%), indicating a possibility that not all of the delta channels flow in one direction from river to bay. Third, flow through transects L1 and L2 ("Old River Cutoff", Figure 6) was always flowing away from the main channel at a rate between about 385 and 574 CFS (11 – 16 m^3/s, 28–41%), which is about half of the flow moving downstream in the Trinity beyond that junction (Figure 8).

It is important to note, however, that measurements at transect D3 in the main channel and transects L1 and L2 in the Old River Cutoff were taken as the tide was still falling, whereas measurements at transect D2 were taken after 1500 CDT when changes in river stage at Wallisville had plateaued (Figure 7). This change in tide may partly explain why there was a mismatch in the water balance at this junction. Ideally, flows would balance to zero:

$$Q_{\mathrm{D1\_B}} + Q_{\mathrm{D2}} = Q_{\mathrm{D3}} + Q_{\mathrm{L2}} \tag{1}$$

However, the left side of Equation 1 sums to 863 CFS (24 m^3/s) while the right side is equal to 1,610 CFS (46 m^3/s). We imagine that additional measurements taken at transect D3 (as well as transects D4 – D11 downstream) after 1500 CDT would yield significantly lower discharges, perhaps less than 350 CFS (10 m^3/s) rather than the 1,000 CFS (31 m^3/s) or so measured during the ebb tide. Furthermore, the CWA was pumping 890 CFS (25 m^3/s, 64%) from the river upstream during this time, which would indicate that the river discharge in the delta could be far less during the flood tide than many of the measured values in Table 1. Lastly, the discharge of 2,530 CFS (72 m^3/s, 180%) measured in the Old River delta channel to the west of the Old River Cutoff (transect L3, Figure 6) is much higher than that in the Trinity River, indicating that this channel conveys a major portion of the tidal prism, perhaps in addition to conveying water that left the Trinity River much farther upstream at Marks Bend.

3.1.3 April 2023 Campaign

Our final ADCP campaign took place on 13 April 2023. On this day, river flows were just beginning to decline from a peak of 28,800 CFS (816 m^3/s) at the Liberty gage, which was the highest discharge in the river since it reached 54,500 CFS (1,540 m^3/s) in May 2021. The data collected during the previous two campaigns provided guidance on the ideal measurement locations for this campaign. The high discharge meant that it would likely be worthwhile to collect data at a few locations farther upstream than what had been collected previously. However, the surprising flow dynamics observed at the junction south of Wallisville (transects D1, D2, D3, L1, and L3 in Figure 6) in October 2022 led us to measure these locations once more, this time during the higher flow conditions.

The most upstream measurement (transect 1, Figure 9) was located several river bends upstream of the CWA pump station, while the most downstream measurements were located near the Old River Cutoff as described above. Transects were positioned such that measurements were taken before and after each discrete location where flow exchange between the river and floodplain was evident or where it is known from the lidar data that floodplain channels exist. The first measurements were taken downstream of Wallisville, at the five locations indicated in Figure 6, between 0830 and 0930 CDT just before low tide. Measurements were repeated at these five transects at the end of the day just before high tide, between 1705 and 1750 CDT. Measurements at the upstream transects began at transect 1 at 1050 CDT and ended at transect 25 at 1645 CDT. The tide was moving in during the time it took to take measurements at transects $1-25$, and overall discharge in the river was just beginning to fall (Figure 3D). Note that the Liberty gage is 8 river miles upstream of transect 1 and 23 river miles upstream of transect 25, and thus the rate

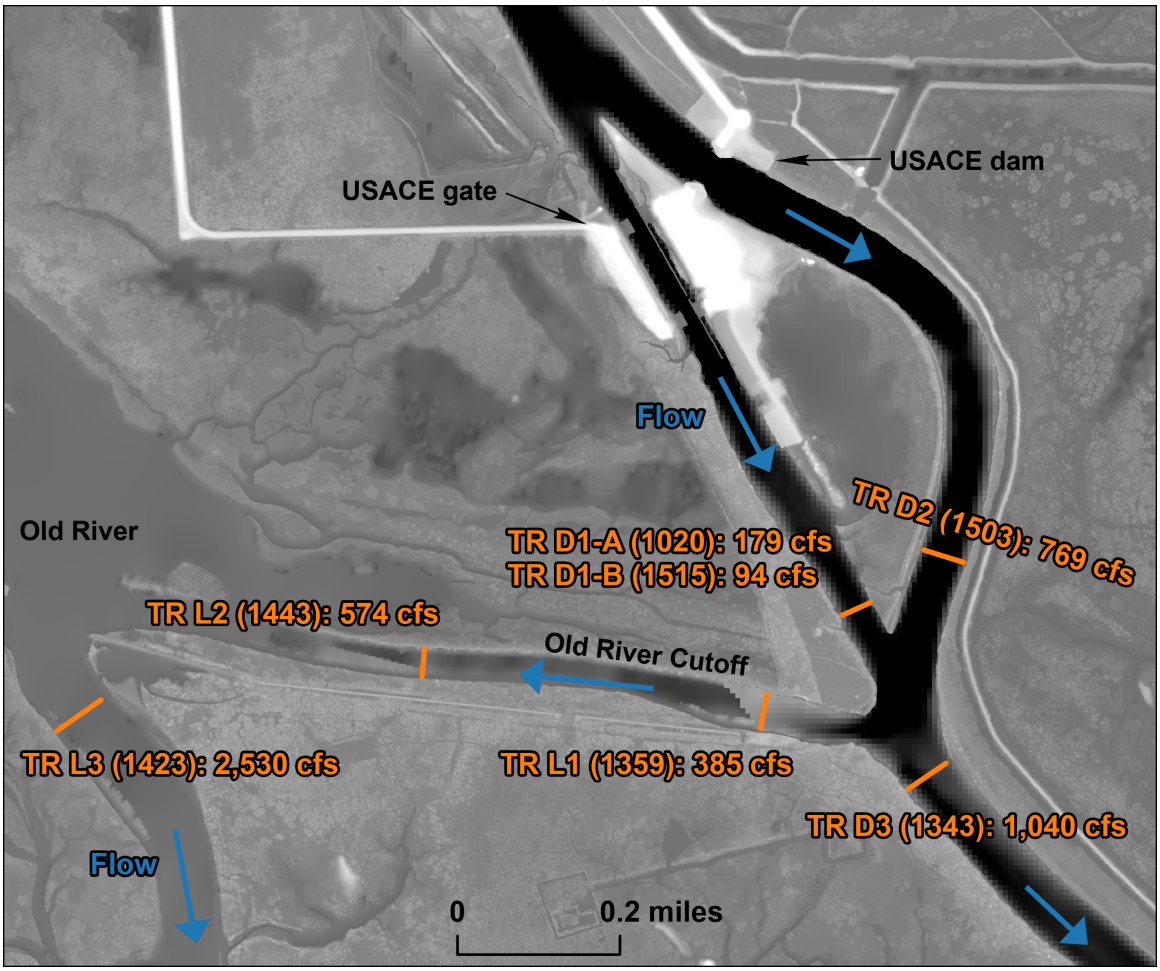

Figure 8: Measured discharges near Wallisville and the Old River on 20 October 2022. Number in parentheses is the approximate time (CDT) when the measurements were taken. See Figure 7 for relationship between time of measurement and tide.

of change of river discharge over the course of 13 April was not as drastic in the study area as indicated in Figure 3D due to the lag time of about eight hours between Liberty and the study area. Still, river discharge was indeed decreasing throughout the day, and therefore measured discharges should be analyzed within this context.

Discharge data collected on 13 April 2023 are shown in Figure 10 as a function of distance downstream, while much of the following discussion of the data is summarized spatially in Figure 11. Similar to the flow patterns observed in May 2022 under lower flow conditions, the most evident change in discharge occurs before and after the Cutoff channel between transects 20 and 21, a change of 2,530 CFS (72 m^3/s, 12%). This discharge through the Cutoff channel is more than twice the value measured in May 2022, even though the main channel discharge at Liberty was only 60% more than the Liberty discharge during the May 2022 campaign. In fact, woody debris that had piled up on one side of the entrance of the Cutoff in May 2022 (Figure B.1) was now completely blocking the channel, rendering the Cutoff impassible by boat (Figure B.2). Unlike the May 2022 measurements, though, during this final campaign there were many more locations of flow loss to the floodplain — and flow return to the river — beyond just the Cutoff. Between the most upstream transects $1-3$, there are two large floodplain channels that connect the floodplain and

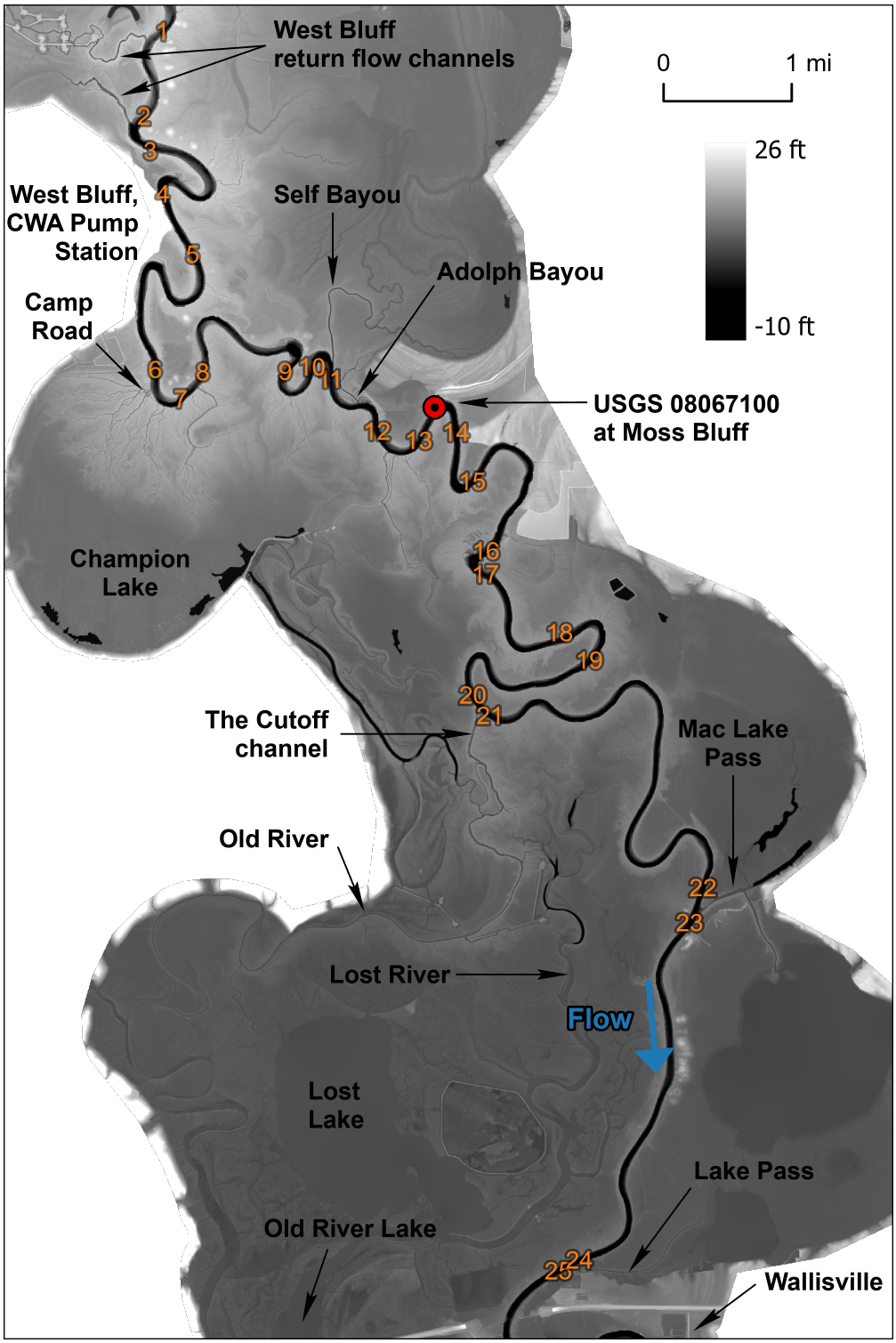

Figure 9: Location of ADCP transects taken during the field campaign in April 2023. Transect locations south of Wallisville and listed in Table 2 are shown in Figure 6.

river just upstream of the bluff where the CWA pump station is located (referred to herein as "West Bluff", see Figure 9 for location and Figure A.1 for aerial imagery). Because measurements were taken during the falling limb of the hydrograph, both channels were conveying flow to the river at rates of 467 and 803 CFS (13 and 23 m^3/s, 2 and 4%), respectively. These measurements provide an example of how a topographic bluff that

encroaches upon the river (such as West Bluff) acts as a discontinuity in the floodplain and forces flow to return to the river. Similar observations are made at all three bluffs in the system, and are supported by model results as discussed in Section 4. Before and after transects at West Bluff and the CWA pump station (transects 4 and 5) showed virtually no change in discharge, even though the pumps were on and running at 950 CFS (27 m^3/s). It may be that the pump station inlet is somewhere farther upstream, which could be explained in part by the flow reduction of 405 CFS (11 m^3/s, 2%) between transects 3 and 4.

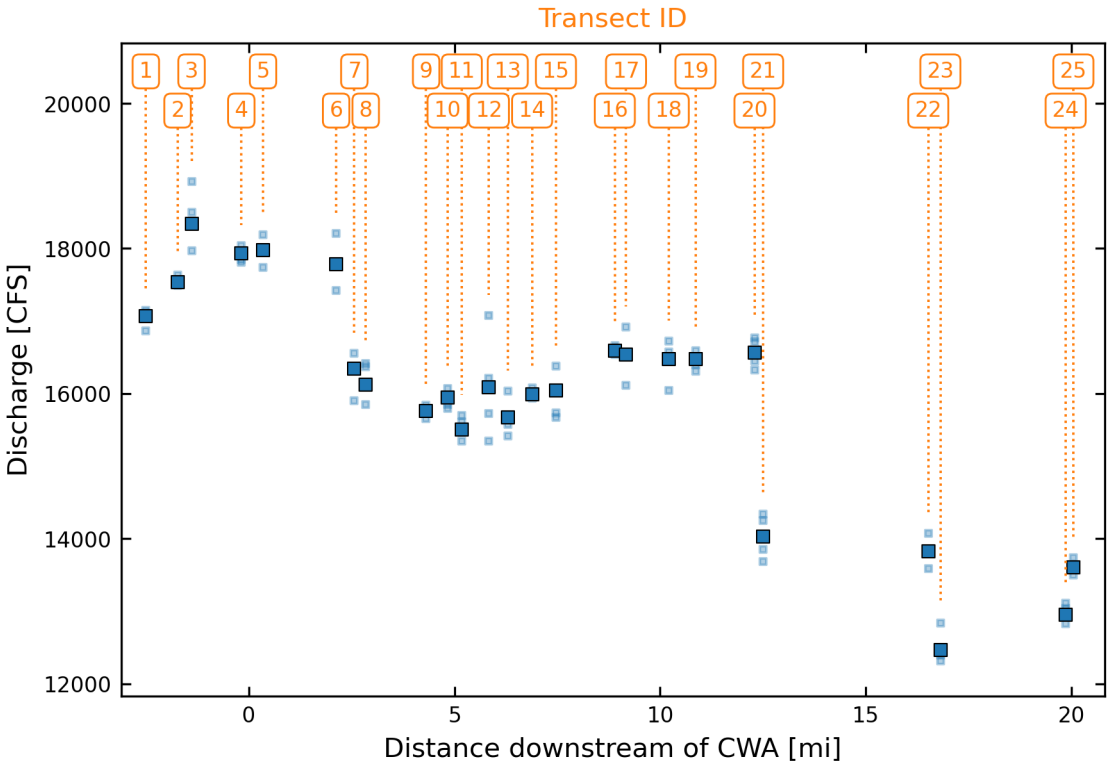

Figure 10: River discharges measured at each transect visited on 13 April 2023, with transect labels shown at the top corresponding to those in Figure 9). The lightly colored markers indicate individual measurements, while the solid, larger markers indicate the mean value. The reference discharge at the Liberty gage during the early hours of 13 April was 21,000 CFS (590 m^3/s).

Another major flow exchange was occurring at Camp Road between transects 6 and 7 (Figure 9). Although ADCP measurements were not taken here in May 2022, we did observe under those discharge conditions the river stage as it had just barely reached above the bottom elevations of the Camp Road floodplain channels. In April 2023, these channels were inundated with an estimated 3 to 6 feet of water depending on the depth of the channel (Figure B.3), and were conveying 1,440 CFS (41 m^3/s, 7%) from the river to the floodplain, based on the data shown in Figure 10.

Downstream of Camp Road, changes in discharge were less drastic but still notable. Discharge decreased by 444 CFS (13 m^3/s, 2%) at transect 11, just downstream of Self Bayou (Figure 9). Then, discharge increased again by 589 CFS (17 m^3/s, 3%) at transect 12, just downstream of Adolph Bayou (although our measurements at transect 12 had more variance than the others nearby). At transect 13, there was a flow decrease of 422

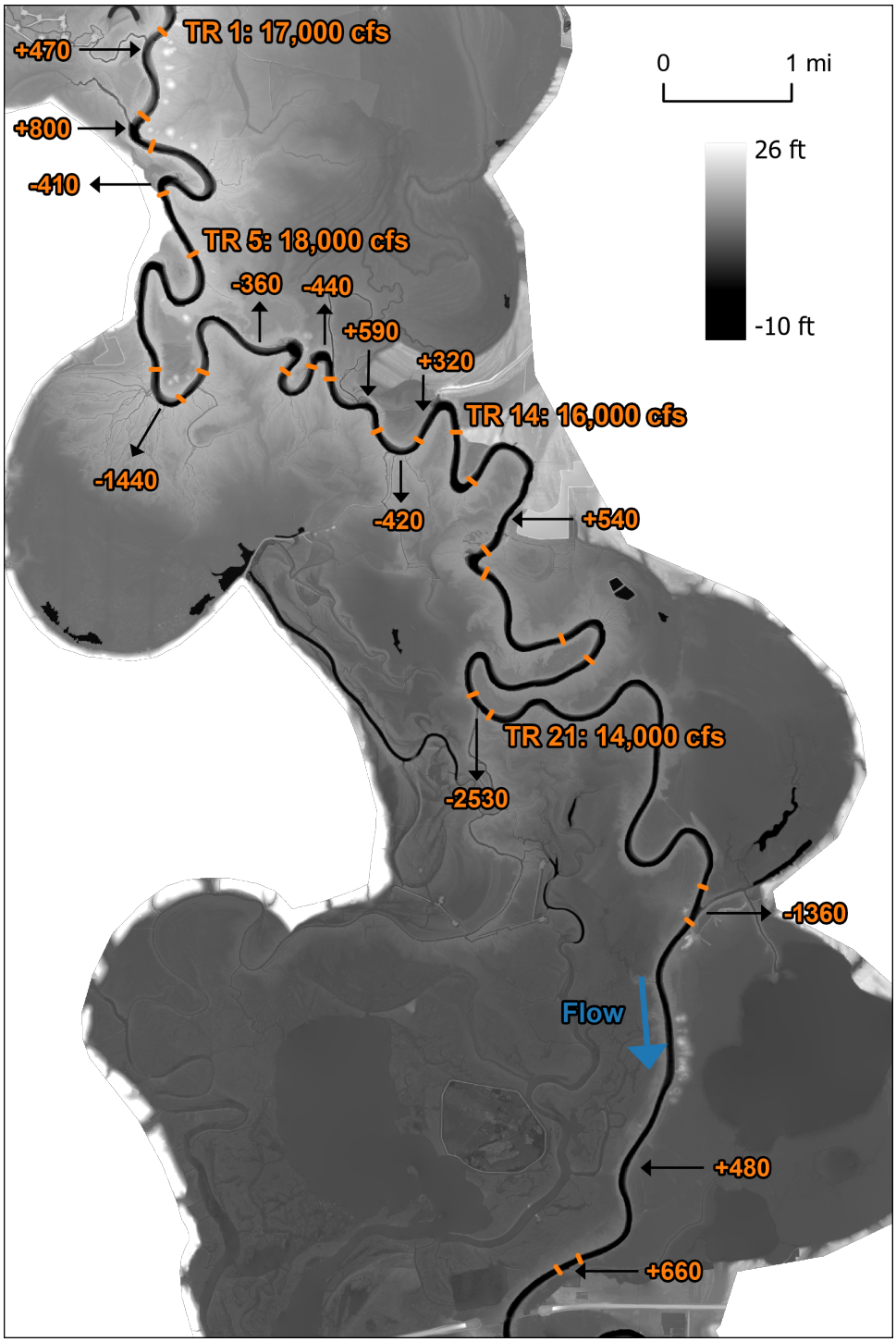

Figure 11: Locations of discharge flux to and from the river based on the measured ADCP data. For simplicity, only major fluxes are shown. All discharges in units of CFS.

CFS (12 m^3/s, 2%) that corresponds to the set of deep and narrow floodplain channels located at the bend between transects 12 and 13. Finally, discharge increased by 320 CFS (9 m^3/s, 2%) at transect 14 downstream of the Moss Bluff pump station and gage (USGS 08067100). This increase is somewhat surprising, as the presence of the pump station and canal here might indicate a decrease in flow. However, we do not have the data to know how much water was being pumped at this site, if any. It is also likely that the floodplain just upstream of the Moss Bluff pump station (on the same side) was

introducing flow back into the river, as this part of the floodplain is low-lying and was completely inundated during data collection (Figure B.4). This flow increase upstream of Moss Bluff is another example of how the bluffs along the river control return flows from the floodplain.

There was another surprising flow increase of 543 CFS (15 m^3/s, 3%) between transects 15 and 16, which is larger in magnitude than those described above but cannot be explained by any visibly connected water bodies. There is a small community on the east bank of the river between these transects, including an engineered lake behind it, but it is not clear how or how much water could be entering the river through this community.

Downstream of the Cutoff, we took measurements before and after Mac Lake Pass and Lake Pass, as we did in May 2022. The flow directions were similar, but the magnitudes of the fluxes were considerably larger than those measured during the first campaign. Also similar is the return flow occurring *between* the two passes, which in April 2023 was measured at 482 CFS (14 m^3/s, 2%). In fact, at many locations near and upstream of Lake Pass we observed floodplain water trickling through the forest back into the river. This floodplain and riverbank was similar to the one observed upstream of Moss Bluff (Figure B.4) in the sense that the bank is so low-lying that it was completely inundated, and it is located just upstream of a major bluff that forces floodplain water to return to the river.

Discharge measurements were also taken downstream of Wallisville during this campaign, in parts of the main channel and delta where tides become important (Figure 6, Table 2). Measurements were taken at five locations in the morning (transects "-A"), and were repeated in the late afternoon (transects "-B") of 13 April. In the morning just before low tide, of the combined 15,300 CFS (435 m^3/s, 73%) that were passing through the Wallisville gate (transect D1) and dam (transect D2), 11,200 CFS (317 m^3/s) moved through the Old River Cutoff (transect L1), while the rest continued down the main Trinity River. Such an uneven flow split is surprising considering the majority of river flow is taking a 90-degree turn to the right rather than continuing relatively straight through the main channel. The large conveyance of the Old River Cutoff relative to the Trinity River was observed during the October 2022 campaign, but at much lower flows. During this period of low tide, the majority of the flow in the Old River Cutoff was then turning left and flowing into the Old River delta channel (transect L3).

Perhaps the most interesting finding of these delta measurements was in the Old River delta channel as we took measurements in the afternoon just prior to high tide. While a flow of 10,700 CFS (303 m^3/s, 51%) moved through this channel toward Trinity Bay in the morning at low tide, the high tide measurements revealed a flow of 1,440 CFS (41 m^3/s) moving *out of* Trinity Bay and into the Old River Lake. At this time, only 3,320 CFS (94 m^3/s, 16%) were continuing down the main channel of the Trinity River. These two channels are by far the largest delta channels, which implies that even under high river discharge conditions the vast majority of river flows are being stored in the system of floodplain channels and lakes between Wallisville and Moss Bluff during the flood tide.

3.2 Floodplain Instrumentation

In addition to collecting ADCP data, during our May campaign we placed pressure transducers (for water depth measurement) and tilt current meters (TCMs, for velocity

Table 2: Discharge measured at each transect visited in the Trinity River delta on 13 April 2023, with transect labels corresponding to those in Figure 6 (all discharges in units of CFS). Mean discharge values are shown spatially in Figure 12. The reference discharge at the Liberty gage during the early hours of 13 April was 21,000 CFS (590 m^3/s).

Transect	Time (CDT)	No. Measurements	Mean	Min	Max
D1-A	0930	2	5710	5700	5720
D2-A	0920	2	9640	9630	9650
D3-A	0905	2	3680	3550	3810
L1-A	0850	3	11200	11100	11400
L3-A	0830	4	10700	10400	11000
D1-B	1705	2	4910	4810	5010
D2-B	1720	2	8620	8520	8730
D3-B	1730	2	3320	3280	3360
L1-B	1740	2	9880	9880	9890
L3-B	1750	3	-1440	-1480	-1340

measurement) at six channelized locations (Sites $1-6$) in the floodplain between Marks Bend and Camp Road (Figure 13). Figure C.3 shows an example of how the instruments were secured together. The TCM becomes buoyant when the channel is inundated and it tilts in the direction of the flow, allowing us to calculate the flow velocity. Therefore, it must be secured to the ground, and for this purpose we used square concrete step stones of dimensions 12 in. x 12 in. x 1.5 in. We drilled holes in the center of each tile, and fed through and knotted the short rope on the end of the TCM. For each TCM installed, we also installed a pressure transducer alongside it, as the velocity measurements are only valid above a certain depth. The transducers were connected to the tile by threading a copper wire through the center hole, wrapping it around, feeding it through the ring on top of the transducer, and tying the ends of the wire together.

The Site 1 instruments were installed within a depression at a counter point bar, consisting of low-lying deposits that represent a gap in the natural river levee (Figure C.1). Prior modeling efforts (Tull et al., 2022) demonstrated that this river bend can be a preferential flow path when river stage is high but still below bankfull. Site 2 is located in a floodplain channel near the river (Figure C.2), one river bend upstream from the Moss Bluff USGS gage. Site 3 is another floodplain channel connected to the same bend, and is the next channel in the downstream direction from Site 2 (Figure C.3). It is slightly larger than the Site 2 channel, as it is formed by the confluence of three other channels that connect this location to the river bank. Site 4 is located on the same channel as Site 3, about 800 m farther from the river (Figure C.4). The potential benefit of having two sets of instrumentation on the same channel is seeing how flow depth and momentum are reduced with distance away from the river. Lastly, Sites 5 and 6 are located several bends upstream of the others, near Camp Road (Figures C.5 and C.6). At the time of installation in May, the river stage was almost equal to the bottom elevation of the Site 6 channel. In fact, on 13 May we observed water flowing away from the river through one of the larger channels upstream of Sites 5 and 6. The next day, water was no longer flowing there, and instead was flowing back to the river via the Site 6 channel. This flow reversal can be associated with the decrease in river flow shown in Figure 3B between

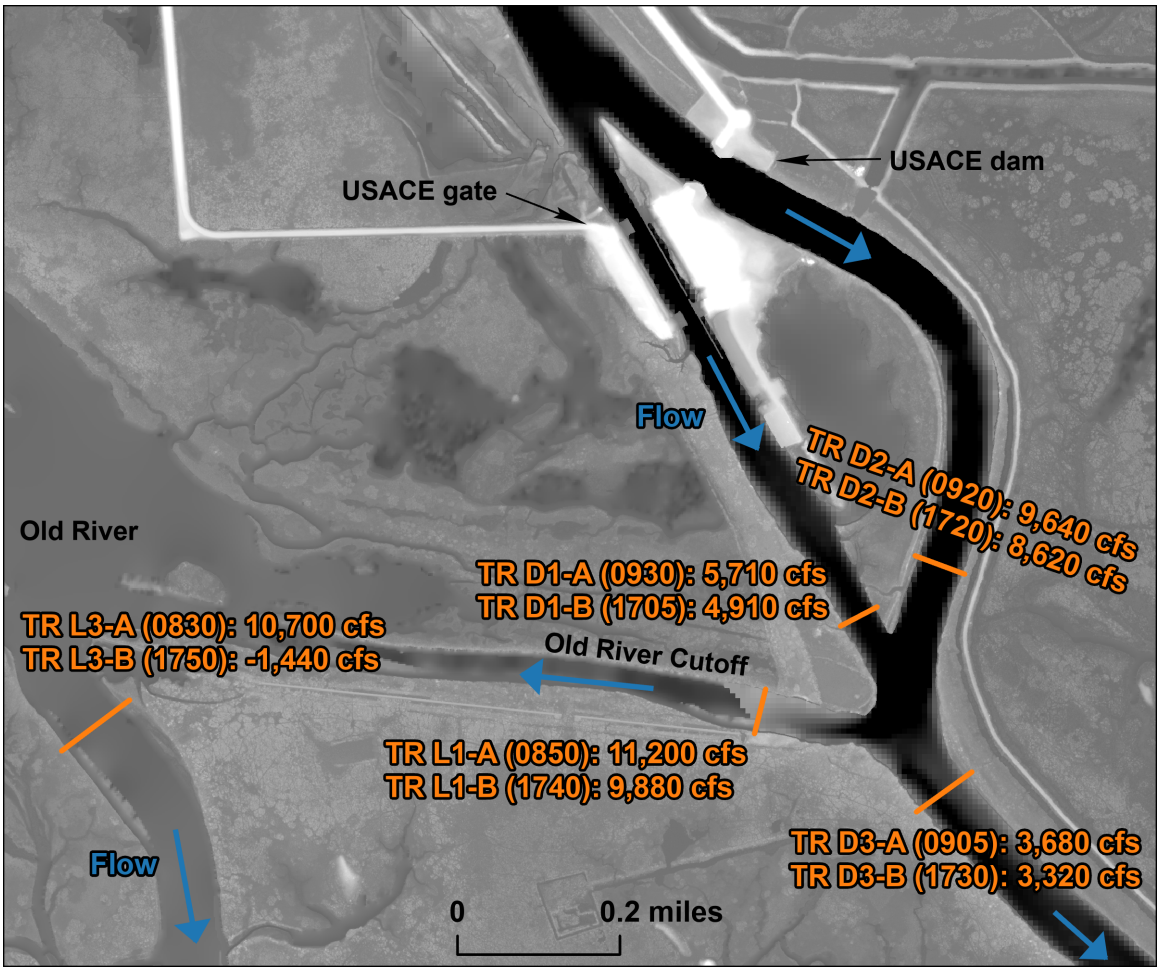

Figure 12: Measured discharges near Wallisville and the Old River on 13 April 2023. Number in parentheses is the approximate time (CDT) when the measurements were taken. The first set of measurements ("A") was just before low tide, while the second set ("B") was just before at high tide.

13 – 14 May.

The instrumented locations in the floodplain represent a variety of channel sizes and floodplain environments. Collecting water depth and velocity data throughout the floodplain will allow us to further calibrate our numerical models of river-floodplain flow exchange and also understand how various river stages translate into water levels and flows into the floodplain. In turn, we hope to extrapolate from these data and the numerical models they inform to get a sense of how much flow moves through the rest of the floodplain channels connected to the Trinity River, and how that compares to the total flow moving through the river and floodplain. Unfortunately, due to the lack of high flow events during 2022, these channels remained dry for the majority of the year. The spring rains of 2023 have brought more flow to the study area, including the partial floodplain inundation observed during the April 2023 campaign. Although this inundation provided good conditions for data collection in the floodplain, we were not able to access the sensors during the campaign because the inundation made the floodplain impassible in some areas. We plan to collect the sensors at the next available opportunity.

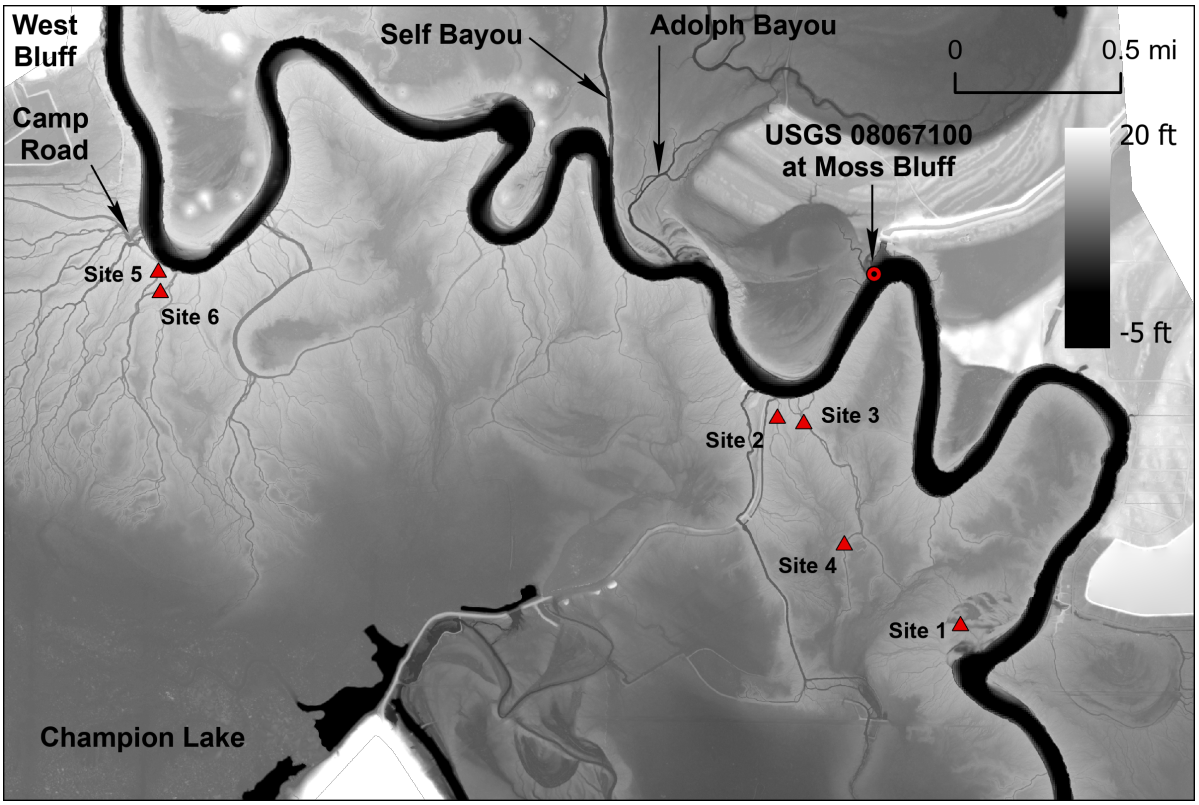

Figure 13: Location of floodplain instrumentation sites used for measuring water depth and velocity within floodplain channels.

4 Further Investigation with Numerical Model

Following our field campaigns, we developed a model that encompasses a larger domain and is calibrated using ADCP measurements. With this new model we are able to analyze patterns of flow exchange between the river and floodplain over longer distances, to see how hydrodynamics change as the river approaches the coast. We also employed a Lagrangian particle routing model that operates in conjunction with the numerical model to track flow paths in and out of the river. The motivation behind this modeling effort is to analyze over a much larger domain a discharge scenario where many of the discussed floodplain channels along the Trinity River actively convey water but river stage remains below bankfull. Model results show how river-floodplain connectivity changes with distance downstream and which river bends are responsible for the most flow exchange between the river and floodplain.

4.1 Model Domain and Setup

The model domain boundary (outline shown in Figure 1) extends from Liberty, TX down to Trinity Bay. We chose Liberty to be the upper boundary because its perched topography provides a natural discontinuity of the floodplain, and because Liberty is the upper limit of the 2017 river bathymetry described in Section 2.1. The east and west boundaries of the domain are aligned with the valley walls, such that the entire floodplain on either side of the river is included. The downstream boundary of the domain is located in Trinity Bay, which allows for a tidal boundary condition to be applied to the model.

Model mesh resolution varies across the model domain, where smaller, complex features are resolved with higher mesh resolution and areas of the floodplain with less topographic complexity are resolved with coarser resolution (Figure D.1). The model domain consists of an unstructured mesh with an average element edge length of 164 ft (50 m) throughout the areas of the floodplain that are unchannelized. In the center of the main channel, the average element size is about 59 ft (18 m), while along the river banks the elements are 39 ft (12 m) in size. To model flows through the numerous floodplain channels in the domain with their various sizes, we first identified channelized areas using filtering rules based on surface elevation, slope, and curvature. Next, we converted the identified channelized areas to polygons, which became breaklines in the mesh. Mesh element spacing along these breaklines ranges from close to 10 ft (3 m) in the smallest channels to about 33 ft (10 m) along the larger channels. In the Trinity Bay, the mesh resolution was relaxed to 660 ft (200 m). The final mesh contains 670,826 elements.

The upstream, left floodplain, and right floodplain boundaries were modeled as no-flow (reflective) boundaries. The downstream boundary in the Trinity Bay is oriented nearly perpendicular to the end of the Trinity River channel and to the major direction of tidal propagation along the bay. Along this boundary, we implemented a time-varying water level condition based on the National Oceanic and Atmospheric Administration (NOAA) predicted tides at Morgans Point in Trinity Bay (NOAA Station ID: 8770613) during the time period of interest. This tide station is located at the mouth of the San Jacinto Bay, some distance from the Trinity River delta, but we chose to apply this tidal signal to our boundary as the best available approximation. The datum of the Morgans Point station is Mean Lower Low Water (MLLW); however, MLLW and NAVD88 differ by less than one inch at this location and so no datum conversion was applied to the boundary condition.

We made several adjustments to the DEM described in Section 2.1 during our model calibration phase. In areas closer to the bay, the floodplain becomes increasingly inundated as it transitions to a delta. However, many of the channels that contain water year-round are "hydro-flattened" in the DEM, where the lidar does not penetrate the water and thus the surface of the DEM is at the elevation of the water surface rather than the channel bed. To improve on this issue in our numerical modeling, we lowered the channel elevations in the DEM based on estimated average water depths in the channel. For the larger channels that had been visited by boat, the estimate was based on depth readings. For smaller channels, the channel lowering was based on visual estimates. We also lowered the bottom elevation of the main channel between Moss Bluff and Trinity Bay, after we picked up depth readings in certain locations over the course of our field campaigns, and found that our DEM bathymetry was not as deep as our measurements would suggest (particularly along this river reach). Furthermore, modeled water levels were consistently too high compared to the USGS gages in the study area. Of course, none of these estimated depth increases represent the "true" bathymetry, but we assume that this manipulation is an improvement in channelized areas where we know the bathymetry is at least somewhat lower.

The DEM was applied to mesh vertices via a least-squares fit with minimal smoothing. Elevations at mesh element centroids were computed as the average of the three vertices, creating a discontinuous, piecewise-constant elevation surface used by the ANUGA "DE0" flow algorithm (Davies and Roberts, 2015). Friction forcing was applied to the domain in

three categories: (1) main channel and other areas below the NAVD88 datum, Mannings $n = 0.02$; (2) floodplain channels above the datum, $n = 0.075$; and (3) unchannelized floodplain, $n = 0.1$ (Figure D.2). These values were chosen based on guidance from literature (Chow, 1959), judgment from field visits and site photographs, and through model testing. The overall Trinity River floodplain, not including the lake and channel networks, is almost entirely forested, and so we opted for a Mannings n distribution based on topography rather than one based on land cover.

4.2 Modeling Discharge from May 2022 Campaign

We tested the model under the conditions of our May 2022 field campaign, when hydraulic connectivity between river and floodplain was incipient in many locations. We applied the discharge hydrograph from the USGS gage at Liberty (Figure 3B) at the upstream end of the domain and ran the model for 10 days, starting on 5 May 2022. We also applied a continuous pumping rate of 890 CFS (25 m^3/s) to the domain to represent flow removal at the CWA pump station, as well as a removal of 530 CFS (15 m^3/s) at the Moss Bluff pump station, which is only a rough estimate. The modeled discharge in the river at day 7.5 of the simulation (corresponding to 1200 CDT 12 May 2022 around when the measurements were made) agrees nicely with the measurements (Figure 14). However, it must be noted that our method of querying the model discharge in the main channel is by drawing a transect over the model grid, consisting of unstructured triangular elements, and calculating the fluxes moving through those elements normal to the transect line. It is a first-order approximation, and computed flow is typically between $1 - 4\%$ higher than the flow that is actually in the river in the model (model water volumes are always conserved). For example, between transects 2 and 4 there is a swing in model discharge of about 400 CFS (11 m^3/s), even though there is virtually no water leaving the river in the model or in the data. Despite the nature of the calculation, the change in flow upstream and downstream of the Cutoff channel (transects $9 - 10$) and in general elsewhere is captured accurately in the model. Comparisons of modeled and measured water levels at the Moss Bluff and Wallisville USGS gages are shown in Figures D.3 and D.4, respectively.

4.3 A Steady Discharge Scenario

After developing the numerical model and comparing to our field measurements, we ran a steady flow simulation to explore how surface-water connectivity between the river and floodplain changes with distance downstream, and which river bends and floodplain channels provide the strongest control on that connectivity. We removed the tidal boundary condition and replaced it with a constant water level boundary condition equal to the average of the tidal range for a one-month period. We ran the model to steady-state for a discharge scenario of 17,700 CFS (500 m^3/s). Modeled depth and velocity grids from this simulation are shown in the Appendix (Figures D.5 and D.6, respectively).

We quantify how the surface-water connectivity between the river and floodplain changes with distance downstream by analyzing each river bend between Liberty and Trinity Bay. We delineated river bank "zones" for each bend, defined as a 660-ft (200-m) buffer from the edge of the river. Within each zone, we calculate the fractional inundated area and the normalized water volume present on the bank. Although these are static quantities (i.e., not fluxes), they provide a sense of how inundation increases downstream, whether or not that is related to actual volumes of water, and which overbank areas generally

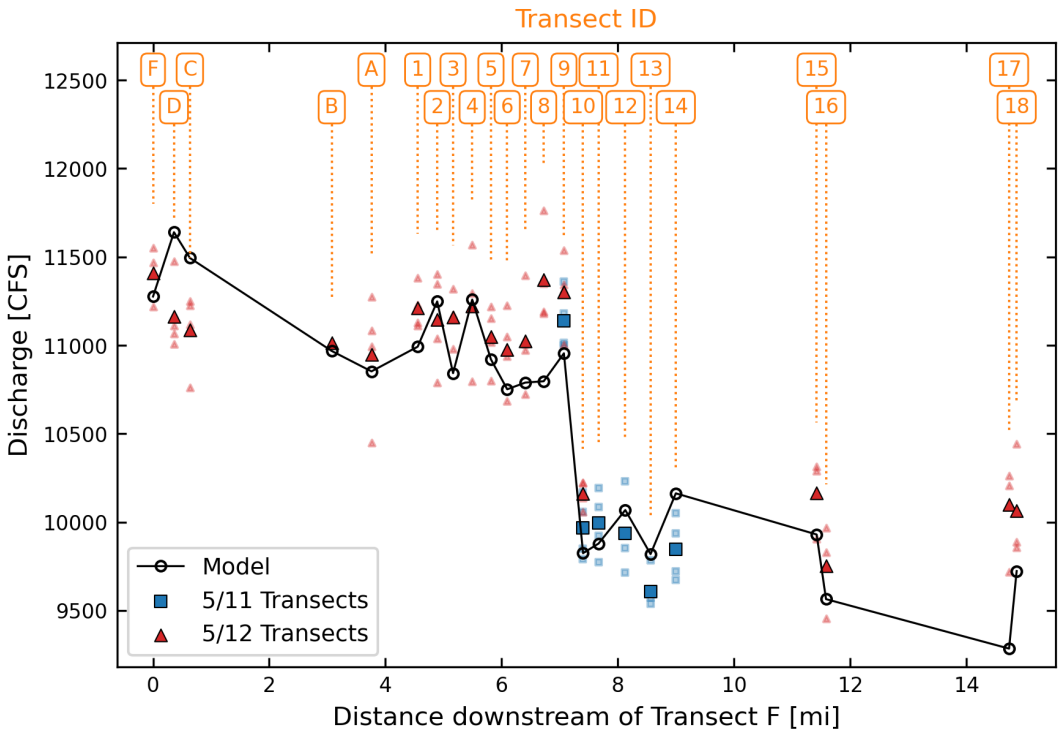

Figure 14: Comparison of modeled to measured river discharge at the transects shown in Figure 4.

hold the most water during medium flow events. The inundated area on each river bend bank increases with distance downstream, which is to be expected as the river transitions to the backwater reach, delta, and bay (Figure 15). Beyond the systematic increase in inundation toward the delta, the bluffs that encroach on the river at three locations (one on the west side and two on the east side, see Figure 1) are major controls on the inundation patterns along the river. In particular, the position of the west bluff (location of CWA pump station) causes a build up of flood waters on the upstream side, whereas on the downstream side (Camp Road area) there is much less inundation.

The volume of water in each river bank zone illustrates the importance of the bluffs to a greater degree than the inundated area (Figure 16). The water volume upstream of each bluff is much higher than elsewhere along the river, and the volume downstream of each bluff is lower than elsewhere. The water volumes on the east and west banks oscillate with distance downstream; that is, there are no locations where water volumes are high on both sides of the river. Perhaps most interesting is the observation that water volumes do not increase with distance downstream, even though the inundated fraction does increase. While this idea may be counterintuitive at first, it can be explained by the fact that there is likely to be more water volume in the floodplain or delta overall, even though there appears to be less water within 660-ft-wide river buffer. These computations within the river buffers can inform on the extent of surface-water connectivity along the river-floodplain interface; however, the results shown in Figures 15 and 16 do not describe the fluxes moving between the river and floodplain.

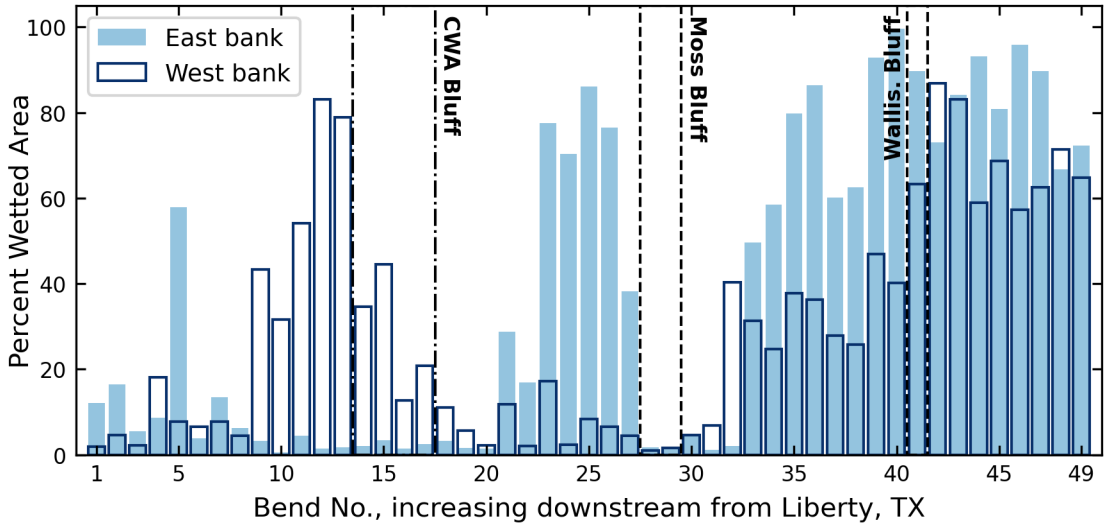

Figure 15: Percent wetted area in each river bend overbank zone. Bend 1 is just downstream of Liberty, TX and Bend 49 is at Trinity Bay. The CWA Bluff is on the west side of the river, while Moss Bluff and Wallisville Bluff are on the east side.

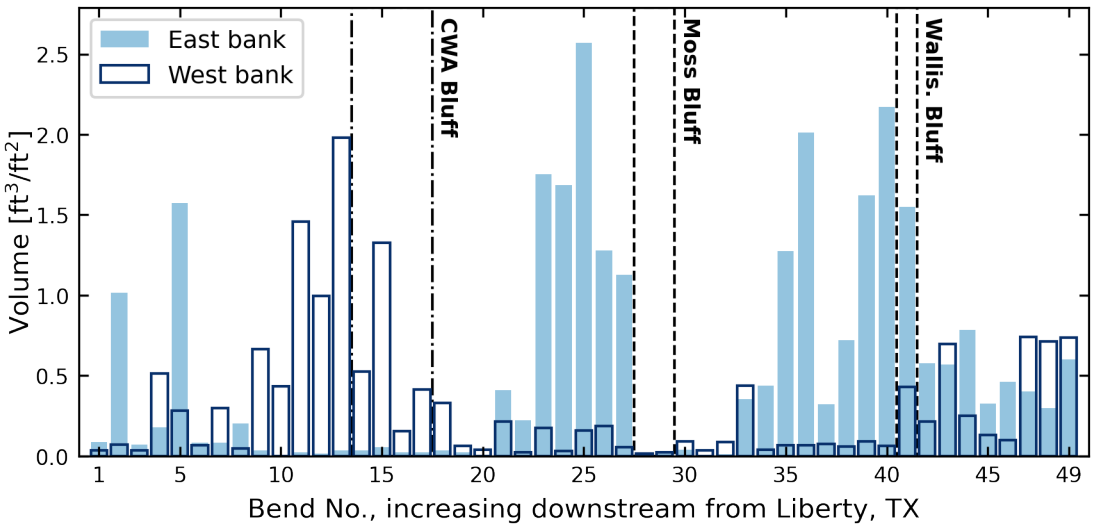

Figure 16: Total water volume in each river bend overbank zone, normalized by the zone area. Bend 1 is just downstream of Liberty, TX and Bend 49 is at Trinity Bay. The CWA Bluff is on the west side of the river, while Moss Bluff and Wallisville Bluff are on the east side.

4.4 Modeling Flow Transport with *dorado*

We used the open-source *dorado* particle routing package for simulating Lagrangian transport through our steady model flow fields (Hariharan et al., 2020). This package is a powerful tool for tracking fluxes and flow paths through a system, and it allows us to quantify fluxes at the river-floodplain boundary and trace those individual fluxes as they flow through the floodplain. *dorado* uses a D-8 random walk algorithm (Pearson, 1905) to simulate passive particle transport through hydrodynamic flow fields, such as those from an ANUGA model. The particle walk algorithm is weighted by local flow direction and

water depth, in a manner similar to that of the DeltaRCM model (Liang et al., 2015a,b). As particles are routed through a flow field, we can track tracks individual paths as well as travel times based on flow velocities in the numerical model, such that at the end of a simulation we know the coordinate position of every step taken by a particle and the travel time associated with that step. The coupled ANUGA-*dorado* approach has been used in several recent studies to model water and material transport (Hariharan et al., 2023; Tull et al., 2022; Wright et al., 2022a).

The ANUGA model depth, stage, and momentum outputs from the model were interpolated to a raster grid at 33-ft (10-m) resolution. We tested the sensitivity of the results to various grid spacings, and found that 33 ft was a sufficient resolution and the computations more feasible. A "cohort" of 100,000 particles was initialized at the upstream boundary of the domain. Particles that remain in the river and do not travel to the floodplain move relatively quickly to the bay ($1 - 2$ days), whereas particles that enter the floodplain move slowly and can in some cases take longer than 30 days to complete their journey. Particle travel times were capped at 30 days, though, as only a small fraction of the 100,000 particles remained in the floodplain after that time.

A few example snapshots of particle positions as they move through the model flow grid are provided in the Appendix (Figures D.7, D.8, and D.9). We computed particle fluxes through each river bank zone, where positive flux indicates flow out of the river and negative flux indicates flow returning to the river (Figure 17). At a discharge of 17,700 CFS (500 m^3/s), fluxes are limited to bends with the lowest levees or deepest floodplain channels. A significantly greater fraction of particles pass through the delta channel downstream of the last bluff (Bend 43, Old River Cutoff) compared to locations upstream, as there are a limited number of locations upstream where fluxes can occur and the delta channels are fairly deep regardless of discharge. We also see that the bluffs are controlling the fluxes. In particular, we note that return (negative) fluxes occur mostly at river bends at or just upstream of the bluffs. By comparing Figures 16 and 17 we observe that locations of high water volume along the river bank correspond to locations of high negative flux but not positive flux. For example, upstream of the first bluff on the east bank (Moss Bluff, Figure 1) there are river bends with relatively high return fluxes (e.g., Bend 27), and this location marks a high point in both inundated area and volume. Alternatively, at Bend 18 (Camp Road) there is some flux moving to the floodplain even though the bank zone at this bend holds a relatively small volume of water. We conclude from this observation that the heavily channelized levee along the Camp Road bend conveys water to the floodplain at higher velocities than elsewhere in the system, perhaps in compensation for the large volumes of water that returned to the river just upstream of the bluff.

This dataset of *dorado* fluxes provides a unique way of not only determining which bends are contributing the greatest fluxes to the floodplain, but also where those fluxes (particles) end up traveling once they do reach the floodplain. For each river-floodplain particle flux, it is possible to find where that flux re-entered the river, and how much time was associated with that unique travel path. From there, we can compute floodplain residence times as a function of the river bend of origin.

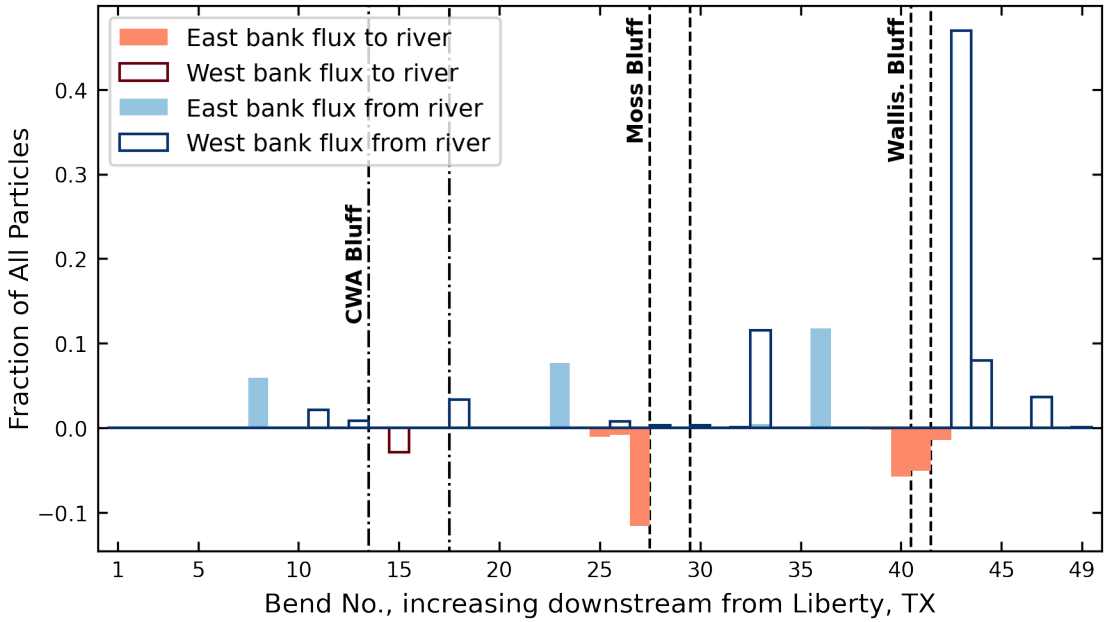

Figure 17: Positive (from river) and negative (to river) fluxes in each river bend overbank "zone". Zone 1 is just downstream of Liberty, TX and Zone 49 is at Trinity Bay. The CWA Bluff is on the west side of the river, while Moss Bluff and Wallisville Bluff are on the east side.

5 Discussion and Conclusions

5.1 The Importance of the Largest Features at Low Flows

Under low flow conditions, the largest floodplain channels are crucial components of the network that connect the river and floodplain. Certainly, the delta passes downstream of Wallisville that connect to the Trinity River at near-perpendicular angles convey water to the bay under all conditions. However, it may not be as much as originally thought. ADCP measurements along the river during the ebb tide showed only small gains and losses of flow upstream and downstream of these passes (e.g., flow gain between transects $5-6$ and flow loss between transects $7-8$, Table 1). Instead, the majority of flow leaving the USACE control structure flows either to the end of the Trinity River or leaves via the Old River Cutoff. The flow measurements in this area indicate that the shortest path to the bay is through the Old River, rather than through any of the delta passes. It is also possible that the passes have blockages; for example, those located between transects $7-8$ were blocked by woody debris on the surface, and there is no telling what the extent of blockage was farther into the passes.

Meanwhile, farther upstream at Marks Bend is the Cutoff channel that measurements indicated to be a significant outflow from the river. Downstream of the location where the Cutoff enters the floodplain, the floodplain becomes increasingly dominated by large floodplain channels and lakes. So although our measurements at the Cutoff were taken while the river discharge was over 10,600 CFS (300 m^3/s), we believe that this channel is an important source of water, sediment, and nutrients to the floodplain even at lower discharges, at the critical location where the river begins to transition into a delta.

5.2 Limited Flow Capacity at the USACE Control Structure

Another important feature of the system is the hydraulic controls at the USACE gate and dam. When the gate is closed, the water levels upstream are raised, which in turn causes more flow to leave the river through the Cutoff channel at Marks Bend. This conclusion is supported by the higher discharge moving through the Old River (Transect L3, Table 1) compared to the main channel, especially at a time when the ebb tide had ceased. Even during higher flows when the gate is open, such as during our May 2022 and April 2023 campaigns, there is some evidence that the hydraulic capacity of the Trinity River is reduced downstream of the USACE structure. We do not know the conditions of the river before this structure and set of embankments were constructed, including whether or not there were any additional distributary channels here. But for a river to be engineered in place over a 4-mile distance where it would otherwise become increasingly connected to its delta, it is possible that the flows moving through the structure here could be higher than they would be under natural conditions. Furthermore, the Old River Cutoff joins the Trinity River at an angle that would suggest a tributary, or at least a bidirectional delta channel. Instead, measurements and modeling results describe this channel as almost entirely distributary, which would indicate an "excess" of flow in the main channel at this location.

5.3 The Role of Smaller Channels at Higher Flows

As the discharge in the main channel increases, more and more floodplain channels begin to activate and convey water and constituents between the river and floodplain. There is a diversity among channel depths, widths, and angles to the main river, such that at medium discharges only the largest floodplain channels and the river banks with the lowest elevation are conduits for surface-water exchange. At river stages that qualify as being well above flood stage, flows to the floodplain are likely to be more evenly distributed along the length of the river. However, the Trinity River levees are highly complex; the increase in levee prominence in the downstream reach can result in the channel banks actually become drier downstream, even though the floodplain may carry more flow. In the backwater reach, the height and width of the levees has resulted in more openings for floodplain channels, whereas in the upstream reach the higher migration rates have created many old relic features like counter point bars, tie channels, and ponds near the river bank that help facilitate connectivity between the river and floodplain. Thus, it is not just the floodplain channels that are important, but also the bends with little to no levee growth or large gaps in the levee (Tull et al., 2022). Ultimately, there are many discontinuities in the river bank elevation and storage spaces in the floodplain, providing opportunities for water to move to the floodplain upstream of the delta, and causing the signature difference between the Romayor and Wallisville USGS gages (Figure 2).

5.4 The Hydraulic Controls of the Bluffs

Data collected during the April 2023 campaign and the model results both show that the bluffs on each side of the river are major driving factors behind the fluxes that occur between the river and floodplain. They may also have an impact on how long it takes water to move through the floodplain. Upstream of all three bluffs in the study area are floodplain basins that are much deeper than most other locations in the floodplain. They have a large capacity to store flood waters, and nutrients that move with the

water through these wetlands experience significant contact time with the ecosystem and wetland soils. Each of these bluffs also has one or two large floodplain channels that conveys flow back into the river. These "forced" return flow locations are deep enough to exchange water between the river and floodplain at both low and high flows, and are undoubtedly important features of a natural system for attenuating flood waves, processing dissolved carbon and nutrients, and maintaining hydrological connectivity year-round. There are many more instances of similar bluffs upstream of our study area, and we imagine that these controls extend to upstream reaches as well.

5.5 Withdrawals at CWA and Moss Bluff Pump Stations

Another major source of flow loss is the continuous pumping of about 920 CFS (26 m^3/s) that occurs at West Bluff by the CWA. This amount is not responsible for the large flow differences seen in Figure 2, but it can be a major fraction of the total river flow at low flows. The USACE gate will likely remain closed under these conditions, and so that pumping would reduce the flow that enters the Old and Lost River lakes via the Cutoff channel. There is also another pump station at Moss Bluff on the east bank (location of the USGS gage), although we do not have data on pumping rates here. This pumping is an important part of the water balance along the lower Trinity River.

A Google Earth Images of Trinity River Floodplain Surface-Water

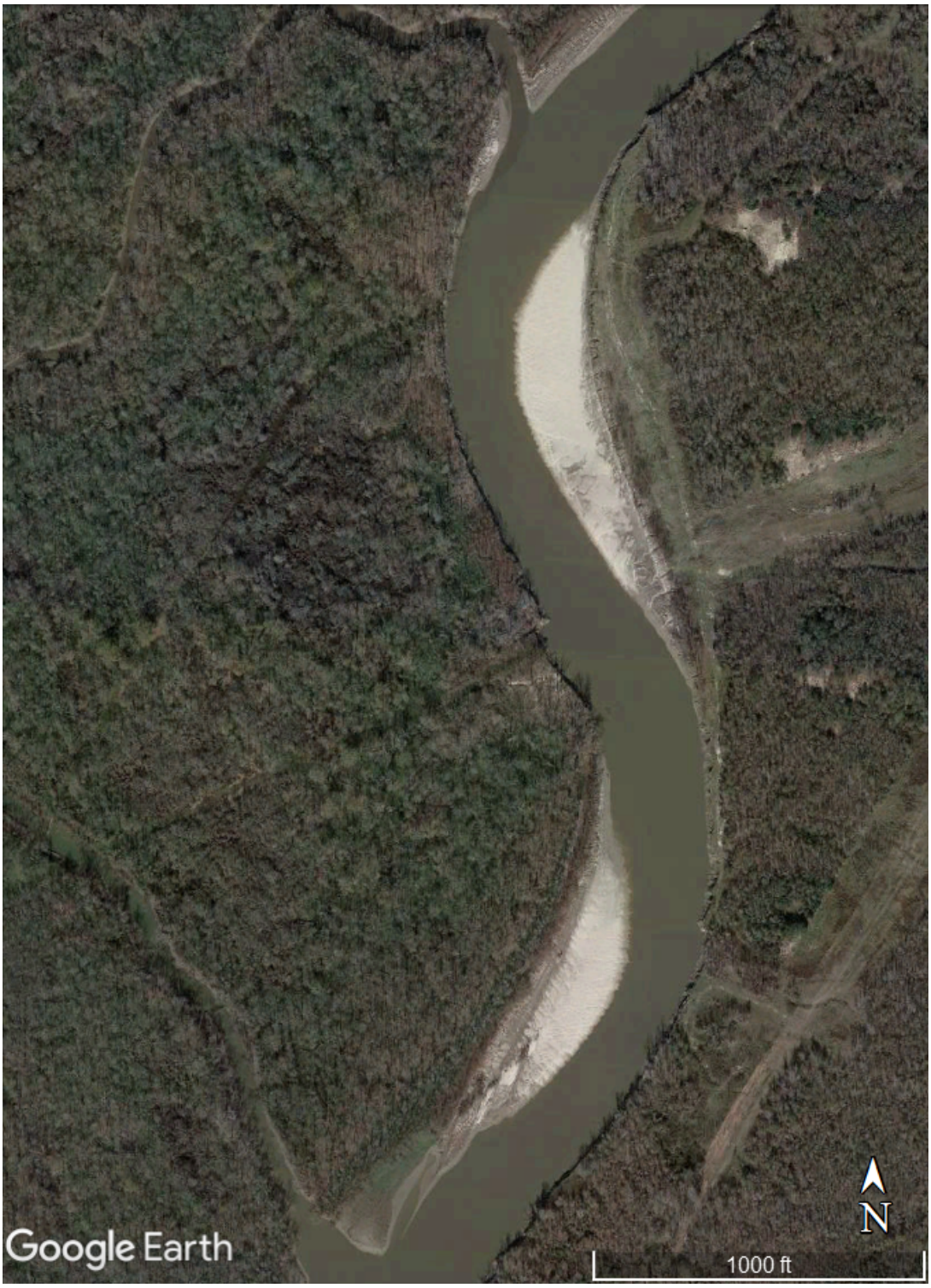

Figure A.1: Aerial imagery showing river-floodplain surface-water connectivity under normal conditions. The two floodplain channels shown here are located just upstream of the West Bluff and CWA pump station (Figure 9).

Figure A.2: Aerial imagery showing river-floodplain surface-water connectivity under normal conditions. The two floodplain channels shown here, Self Bayou and Adolph Bayou, are located just upstream of Moss Bluff (Figure 9).

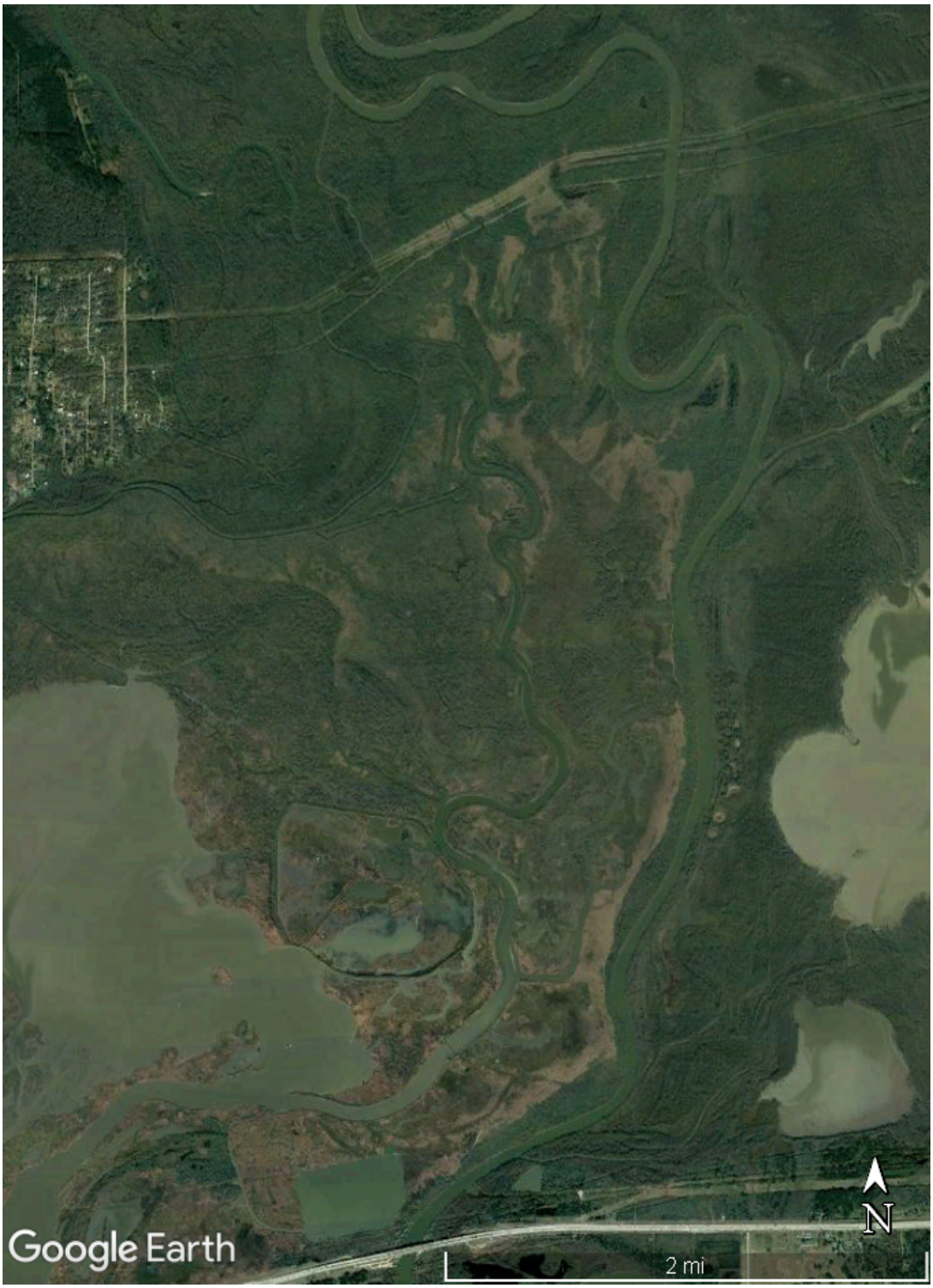

Figure A.3: Aerial imagery showing river-floodplain surface-water connectivity under normal conditions, as the Trinity River approaches the bay. Between Marks Bend at the top of the image and Wallisville and Interstate-10 at the bottom, the floodplain consists of a complex system of channels and lakes.

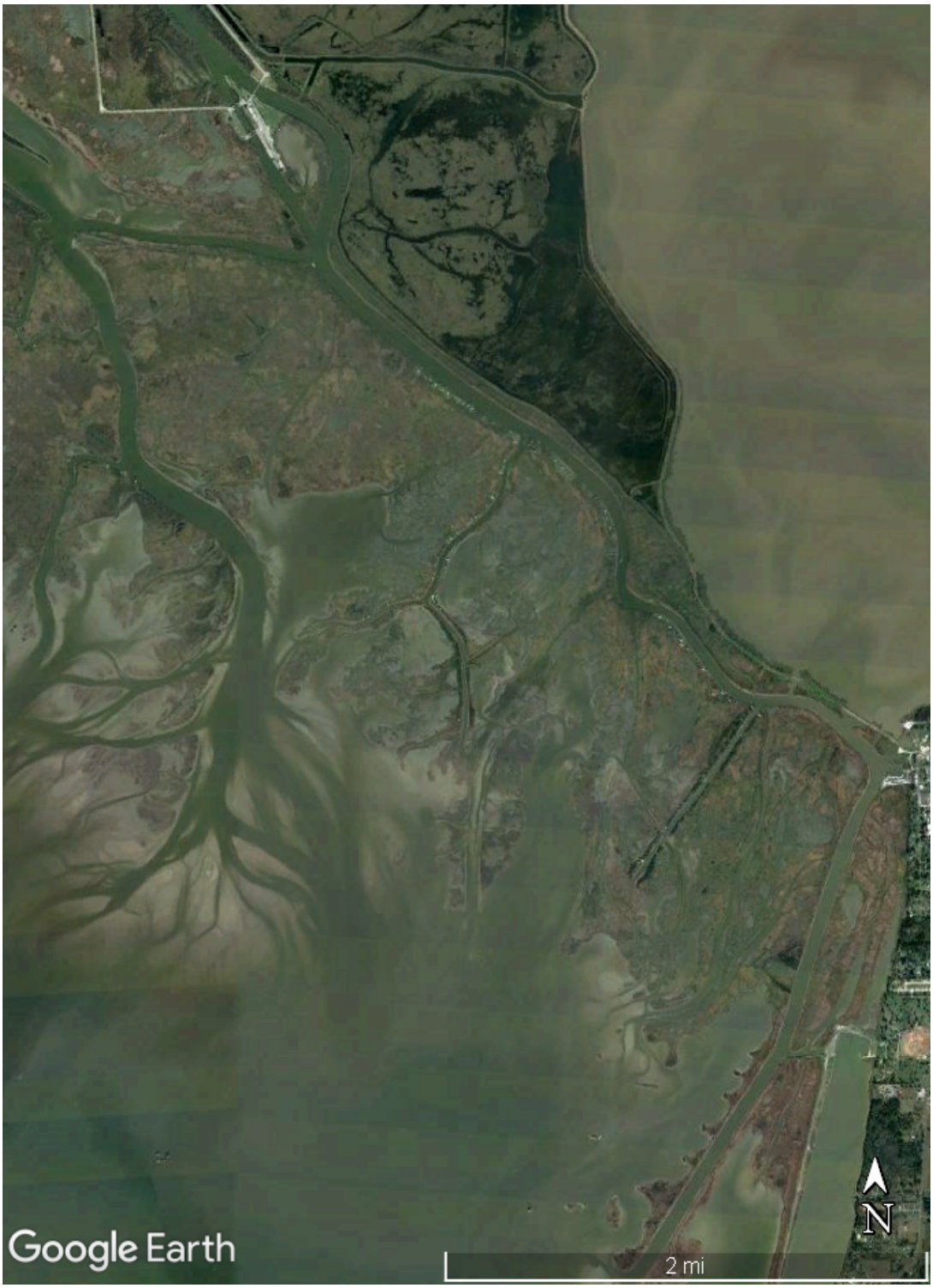

Figure A.4: Aerial imagery of the Trinity River delta, downstream of Wallisville and Interstate-10.

B Photos of Notable Flux Locations Along the River

Figure B.1: The "Cutoff" channel viewed from the Trinity River, where left in the picture is the downstream direction. Flow is moving out of the river through the Cutoff channel (taken May 2022).

Figure B.2: The "Cutoff" channel viewed from the Trinity River, where left in the picture is the downstream direction. More flow is moving through this channel compared to May 2022, and the entire span of the channel is now made impassible by logs (taken April 2023).

Figure B.3: Two large floodplain channels at Camp Road that were inundated and siphoning flow from the Trinity River toward Champion Lake, where left in the picture is the downstream direction (taken April 2023).

Figure B.4: An inundated floodplain forest, located just upstream of the Moss Bluff pump station and USGS gage (located to the right in this picture). Flow is moving slowly into the river from this part of the floodplain (taken April 2023).

C Photos of Floodplain Instrumentation Sites

Figure C.1: Site 1 instrument placement in a shallow basin on a counter point bar (taken May 2022).

Figure C.2: Site 2 instrument placement in a floodplain channel close to the river (taken May 2022).

Figure C.3: Site 3 instrument placement in a floodplain channel close to the river; the same channel as the Site 4 location (taken May 2022).

Figure C.4: Site 4 instrument placement in a floodplain channel farther from the river; the same channel as the Site 3 location (taken May 2022).

Figure C.5: Site 5 instrument placement in a floodplain channel very close to the river. The raised area on the other side of the puddle is Camp Road, and the river is just on the other side of the road (taken May 2022).

Figure C.6: Site 6 instrument placement in floodplain channel farther from the river, but still near to Camp Road (taken May 2022).

D Model Figures

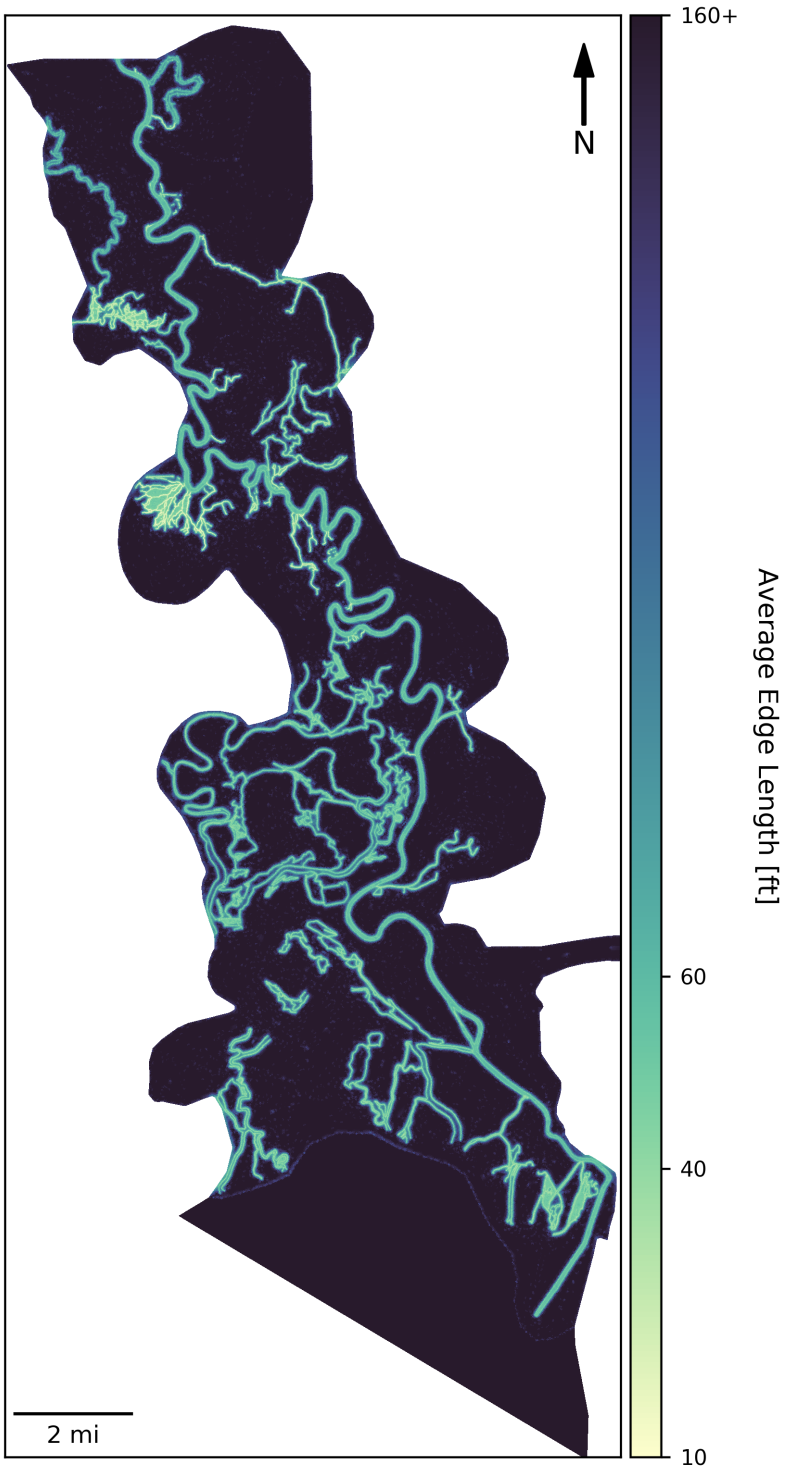

Figure D.1: Distribution of average mesh resolution in the model domain.

Figure D.2: Distribution of mesh friction in the model domain.

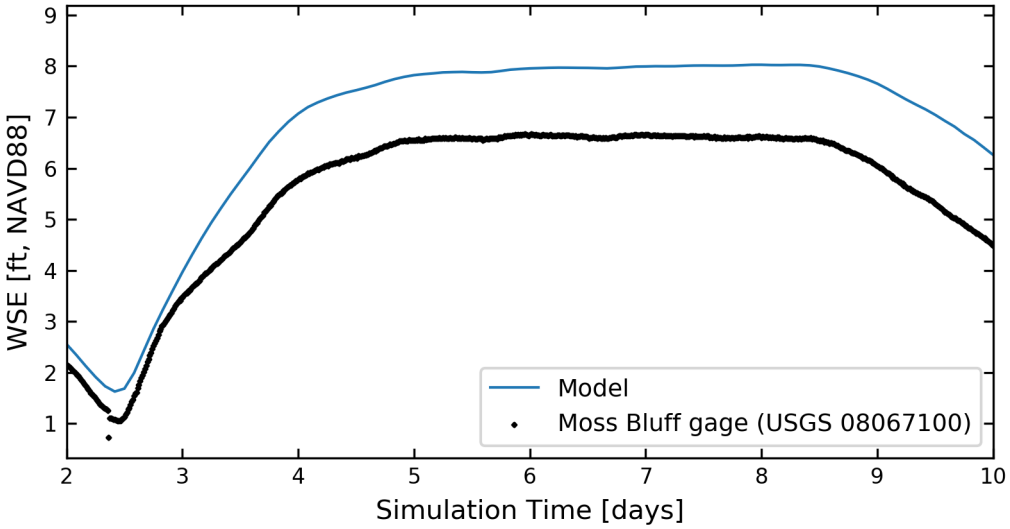

Figure D.3: Comparison of modeled and measured water levels at the Moss Bluff USGS gage.

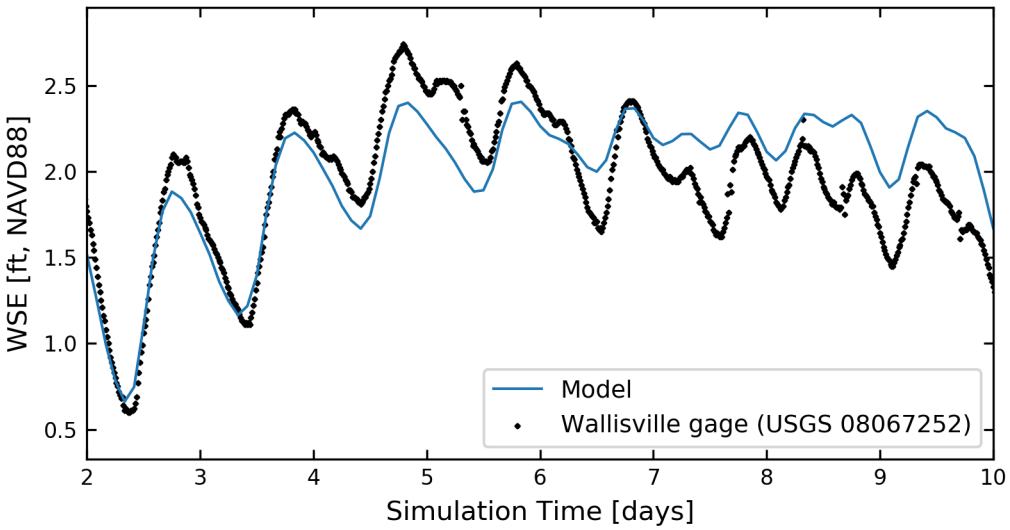

Figure D.4: Comparison of modeled and measured water levels at the Wallisville USGS gage.

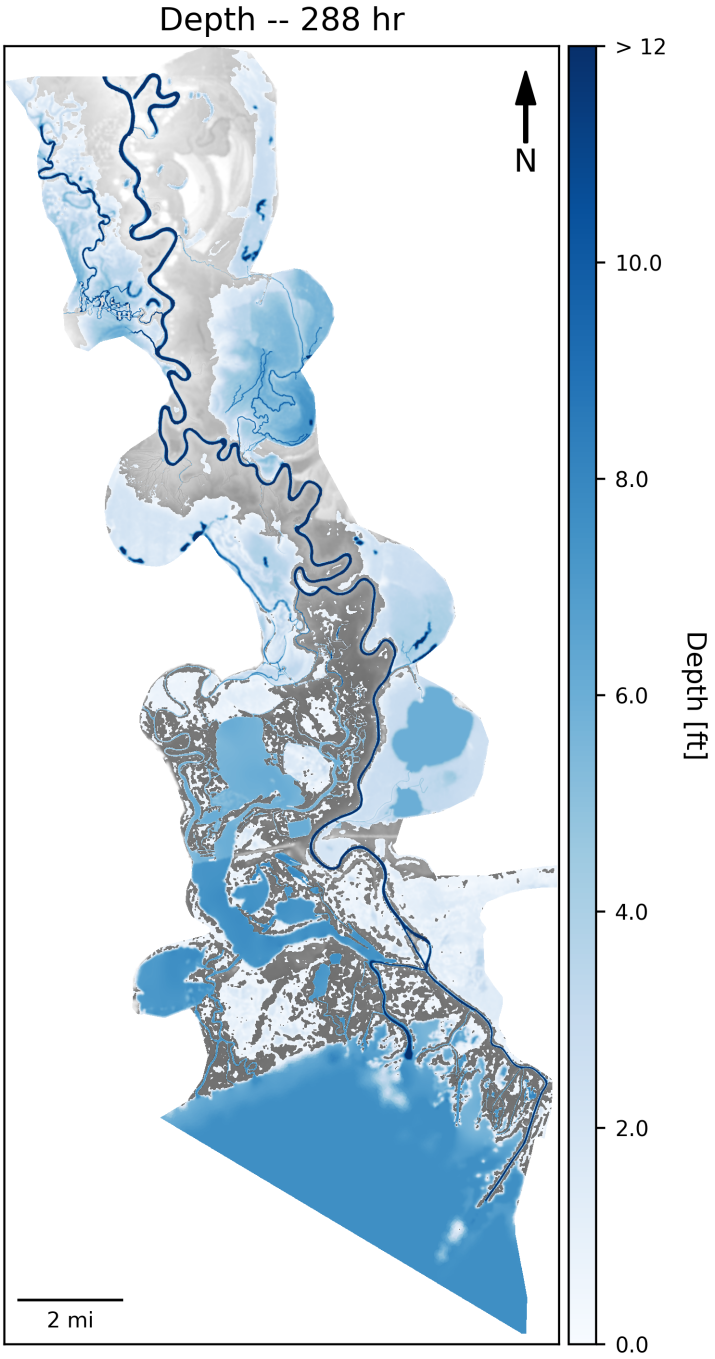

Figure D.5: Modeled water depth at steady Q = 17,700 CFS (500 m^3/s).

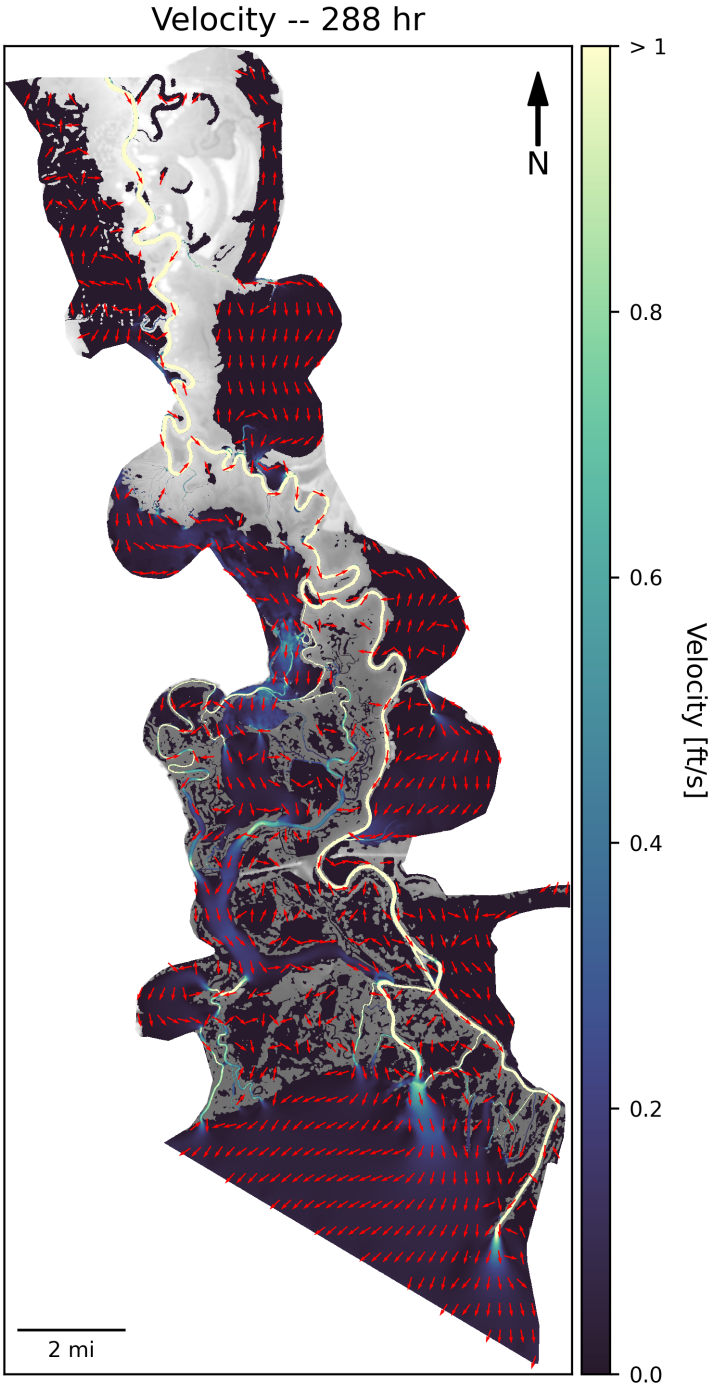

Figure D.6: Modeled flow velocity at steady Q = 17,700 CFS (500 m^3/s).

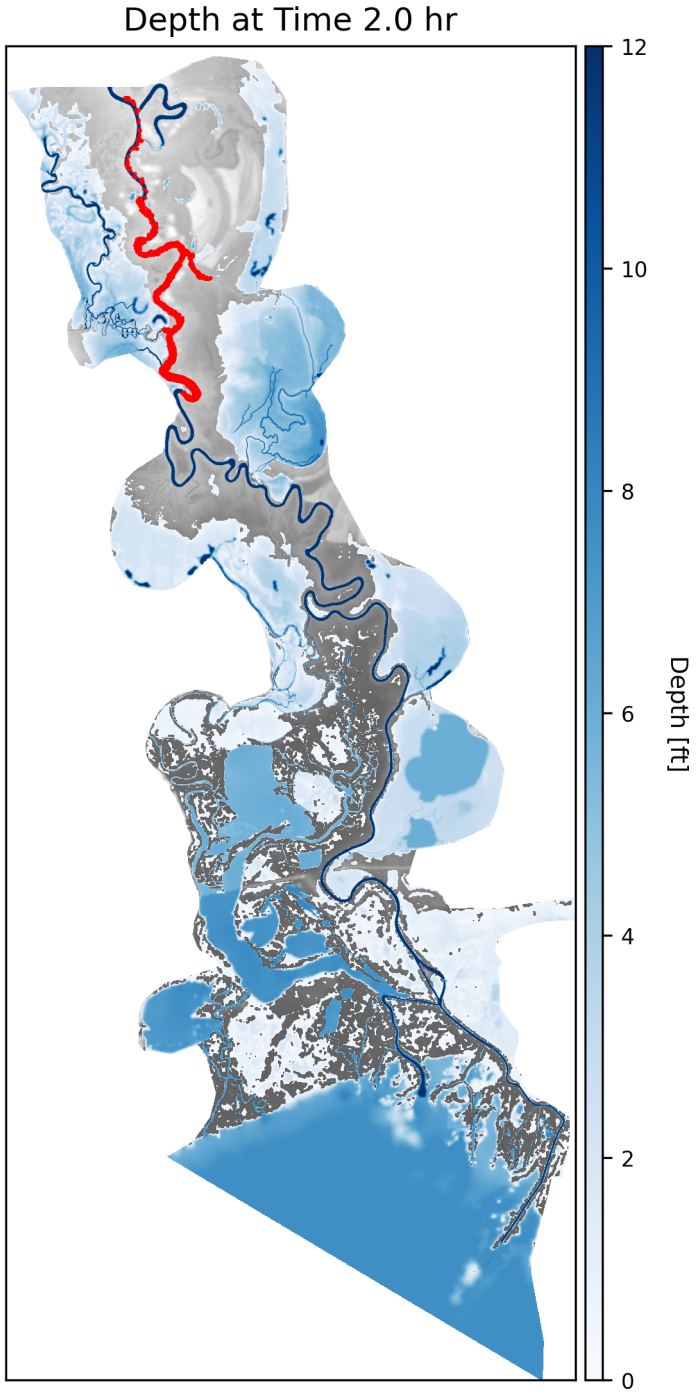

Figure D.7: State of *dorado* particles after two hours of routing through the model flow grid (Q = 17,700 CFS, 500 m^3/s).

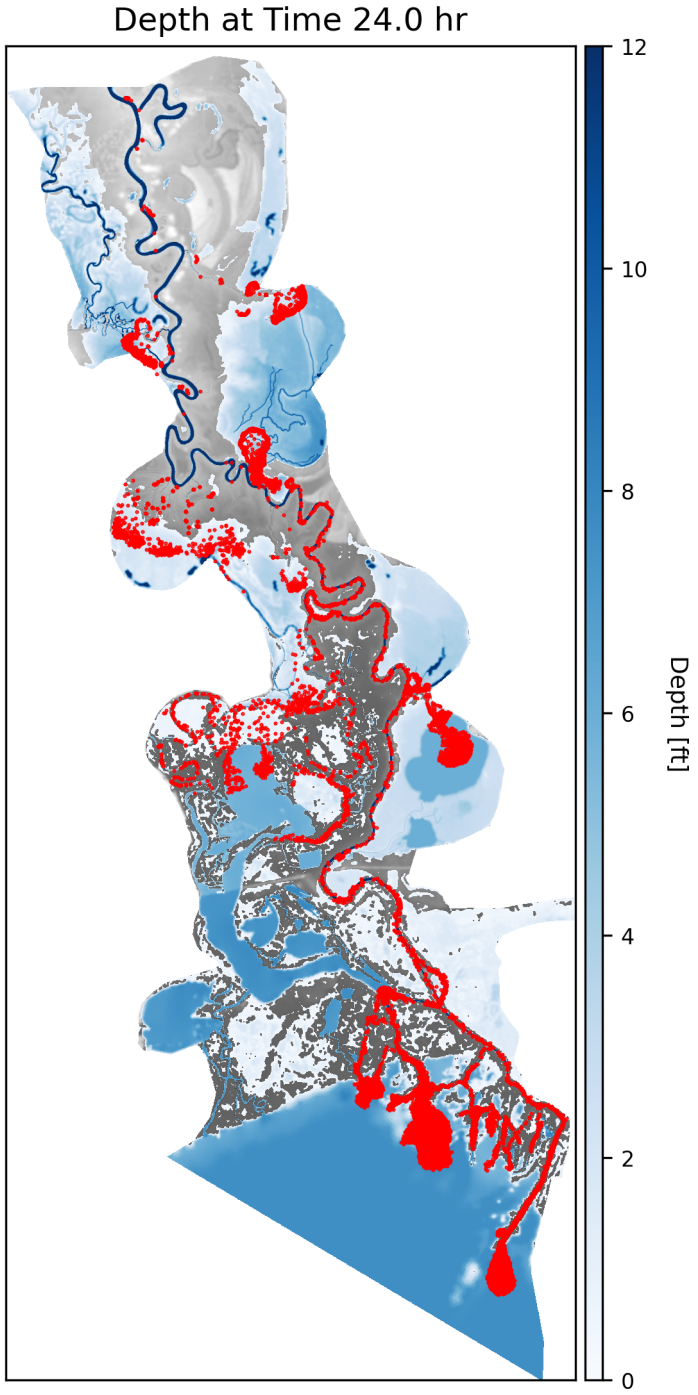

Figure D.8: State of *dorado* particles after 24 hours of routing through the model flow grid (Q = 17,700 CFS, 500 m^3/s).

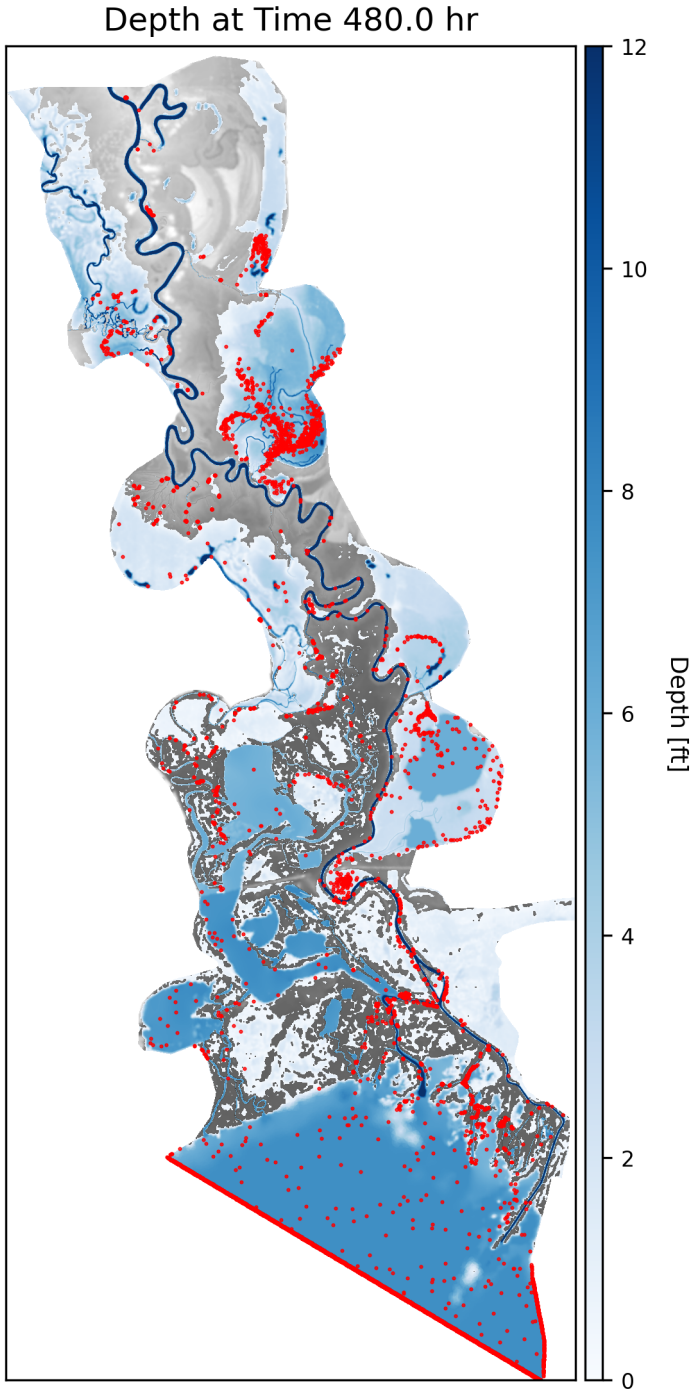

Figure D.9: State of *dorado* particles after 20 days of routing through the model flow grid (Q = 17,700 CFS, 500 m^3/s).

References

Chow, V. T. (1959). *Open-channel hydraulics*. McGraw-Hill Civil Engineering Series.

Davies, G. and Roberts, S. G. (2015). Open source flood simulation with a 2D discontinuous-elevation hydrodynamic model. In *Proceedings of MODSIM 2015*.

Hariharan, J., Wright, K., Moodie, A., Tull, N., and Passalacqua, P. (2023). Impacts of human modifications on material transport in deltas. *Earth Surface Dynamics*, 11(3):405–427.

Hariharan, J., Wright, K., and Passalacqua, P. (2020). *dorado*: A Python package for simulating passive Lagrangian particle transport in shallow-water flows. *Journal of Open Source Software*, 5(54):2585.

Hassenruck-Gudipati, H. J., Passalacqua, P., and Mohrig, D. (2022). Natural levees increase in prevalence in the backwater zone: Coastal Trinity River, Texas, USA. *Geology*, 50(9):1068–1072.

Hiatt, M. and Passalacqua, P. (2015). Hydrological connectivity in river deltas: The first-order importance of channel-island exchange. *Water Resources Research*, 51.

Liang, M., Geleynse, N., Edmonds, D. A., and Passalacqua, P. (2015a). A reduced-complexity model for river delta formation - Part II: Assessment of the flow routing scheme. *Earth Surface Dynamics*, 3:87–104.

Liang, M., Voller, V. R., and Paola, C. (2015b). A reduced-complexity model for river delta formation - Part I: Modeling deltas with channel dynamics. *Earth Surface Dynamics*, 3:67–86.

Mungkasi, S. and Roberts, S. G. (2011). A finite volume method for shallow water flows on triangular computational grids. In *Proc. 2011 Int. Conf. Advanced Computer Science and Information System (ICACSIS)*, pages 79–84. IEEE.

Mungkasi, S. and Roberts, S. G. (2013). Validation of ANUGA hydraulic model using exact solutions to shallow water wave problems. *Journal of Physics: Conference Series*, 423(1).

Nielsen, O., Roberts, S. G., Gray, D., McPherson, A., and Hitchman, A. (2005). Hydrodynamic modelling of coastal inundation. In *Proceedings of MODSIM 2005*.

Pearson, K. (1905). The problem of the random walk. *Nature*, 72(1867):342–342.

Roberts, S. G., Nielsen, O., Gray, D., Sexton, J., and Davies, G. (2015). *ANUGA User Manual*. Geoscience Australia.

Smith, V. B., Mason, J., and Mohrig, D. (2020). Reach-scale changes in channel geometry and dynamics due to the coastal backwater effect: the lower Trinity River, Texas. *Earth Surface Processes and Landforms*, 45(3):565–573.

Tull, N., Passalacqua, P., Hassenruck-Gudipati, H. J., Rahman, S., Wright, K., Hariharan, J., and Mohrig, D. (2022). Bidirectional river-floodplain connectivity during combined pluvial-fluvial events. *Water Resources Research*, 58(3):e2021WR030492.

Wright, K., Hariharan, J., Passalacqua, P., Salter, G., and Lamb, M. P. (2022a). From grains to plastics: Modeling nourishment patterns and hydraulic sorting of fluvially

transported materials in deltas. *Journal of Geophysical Research: Earth Surface*, 127(11):e2022JF006769.

Wright, K., Passalacqua, P., Simard, M., and Jones, C. E. (2022b). Integrating connectivity into hydrodynamic models: An automated open-source method to refine an unstructured mesh using remote sensing. *Journal of Advances in Modeling Earth Systems*, 14(8).